2007

The Effects of Material Treatments on the Surface Properties of Polymeric Biomaterials

Ajoy Vase
Pomona College

The Effects of Material Treatments on the Surface Properties of Polymeric Biomaterials

Physics Senior Thesis

Ajoy Vase, Pomona College
Class of 2007

Advisors:
Prof Elizabeth Orwin
Department of Engineering, Harvey Mudd College

Prof. David Tanenbaum
Department of Physics, Pomona College

Dedication

To my family:

My Dad, Ashok and my Mom, Oreen who have sustained me in my journey through life and college,
My brother Abhinand, who is the reason that I am where I am today
My sister Anjali, who has always searched tirelessly for her lost little brother since he was four,
My brother Abishai, whose mind is as deep and unfathomable as the ocean
My brother Aditya, who has a heart of gold and a spirit of simplicity that I will always treasure.

And my godparents, Virendra and Jean, who stand for everything that I aspire to be.

TABLE OF CONTENTS

Introduction

1.1 Biomaterials and Biocompatibility

Technology and medicine are becoming increasingly connected in research and industry. The boundaries between the traditional sciences, engineering and medicine are growing increasingly dim as researchers identify that engineering, physics and mathematical modeling processes can be applied to find solutions to medical problems. The medical device industry acts as a common interface for interdisciplinary research to take place as scientists, engineers and doctors attempt to develop products to facilitate the recovery of the human body and improve its performance. The entire discipline of biomedical engineering is based on this interface and encompasses research and education in a whole host of sub-disciplines. These sub-disciplines exist across the spectrum of biology and engineering, from drug development and delivery to biomechanics and neural control networks.

The interaction between materials science and medicine is one example of how an engineering discipline interfaces with biological phenomena. Materials are being investigated for their ability to perform within a biological setting. This is not a particularly new development in many respects – upto 2000 years ago, historians believe that gold was being used for dental implants [1]. However, the development of new materials and the realization that they are compatible with other biological systems has led to a significant push in the research and development of biomaterials.

A biomaterial, as defined by Park et al, is a material used to replace part of a living system or to function in intimate contact with living tissue. This contrasts with a biological material, which is directly produced by a biological system. For example, tooth enamel would qualify as a biological material, but a gold filling would be a biomaterial [2; pp1].

The term biomaterial is applied to a number of different substances, from metals to ceramics to polymers. Materials are now being developed with certain properties to address specific problems in the medical field. A number of polymer studies, in particular, were begun with specific medical applications in mind. This movement can be traced back to the 1960's and 1970's when doctors began to campaign for an interdisciplinary approach to medical device design [3; pp2].

When considering the viability of using a certain biomaterial, a study of its biocompatibility is in order. David Williams, a prominent scholar in the field, defined biocompatibility to be the ability of a material to perform with an appropriate host response in a specific application [4]. The compatibility of the material is determined by its mechanical, chemical, surface and pharmacological properties.

Biomaterials, and in particular polymers, are used in a variety of capacities in the medical field [2; pp2]:

i. Therapeutic: biomaterials can be used to replace and repair injured tissues, assist the function of vital organs, or in disposable articles required on a regular basis for treatment.
ii. Drug delivery: biomaterials can be designed to release drugs into the body using different mechanisms and pathways
iii. Diagnostic inspection: as markers, tracers or reagents to detect particular substances or diseases.
iv. Bioengineering: materials can be used to create environments for cell cultures and biological reactions, or for separation of components in bodily fluids, etc.

(Note: There are cases where the nature of the application and the type of material involved means that that a certain material can be useful in more than one of these categories, for example, a certain compound may be synthesized to provide nutritive value to a vital organ, thus fitting the criteria for (i) above, and it might also contain a tracer that tracks its position in the body, which means it falls into category (iii))

This particular study is primarily concerned with the last subfield in this list. Following is a description of the biomedical application that motivates the study carried out.

1.2 The Orwin Research Group: Artificial Cornea Fabrication

The Orwin research group at Harvey Mudd College has been developing a model for an tissue engineered cornea. The need for this device arises from the widespread occurrence of corneal disorders, from inflammations to degeneration to infections. According to Chirila et al, corneal disorders are the second most prevalent cause for blindness in the world [5]. The need for donors far outweighs the current supply, which encourages research efforts to develop an engineered solution [6].

The Orwin group at Harvey Mudd has developed a model by seeding corneal stromal fibroblasts on a 3-D collagen scaffold. In a paper by Shah, Voorhees et al, the authors describe the bioreactor system that they have developed in order to mimic the intraocular pressure on the cornea. In general, a bioreactor is a device that supports or facilitates the working of a biological system. The bioreactor developed by the members of the Orwin group enables them to produce functional corneal equivalents because the cells are manipulated in a setting that emulates in vivo stress conditions [7].

1.3 Bioreactor design

The bioreactor system needs to fulfill a number of different functions [8]. It needs to provide a sterile culture environment for the cells and in addition, be able to stimulate the tissue in a way that can easily be characterized. The bioreactor should also be able to maintain the concentrations of fluid and nutrients in the required proportions in the culture medium. In order to fulfill all these criteria, it needs to be a closed system. It should seal well to prevent fluid leaks and also be easy to assemble so that the chances of contamination are reduced. The bioreactor should also be inert under repeated sterilization and allow for imaging of the contents in the Optical Coherence Microscope.

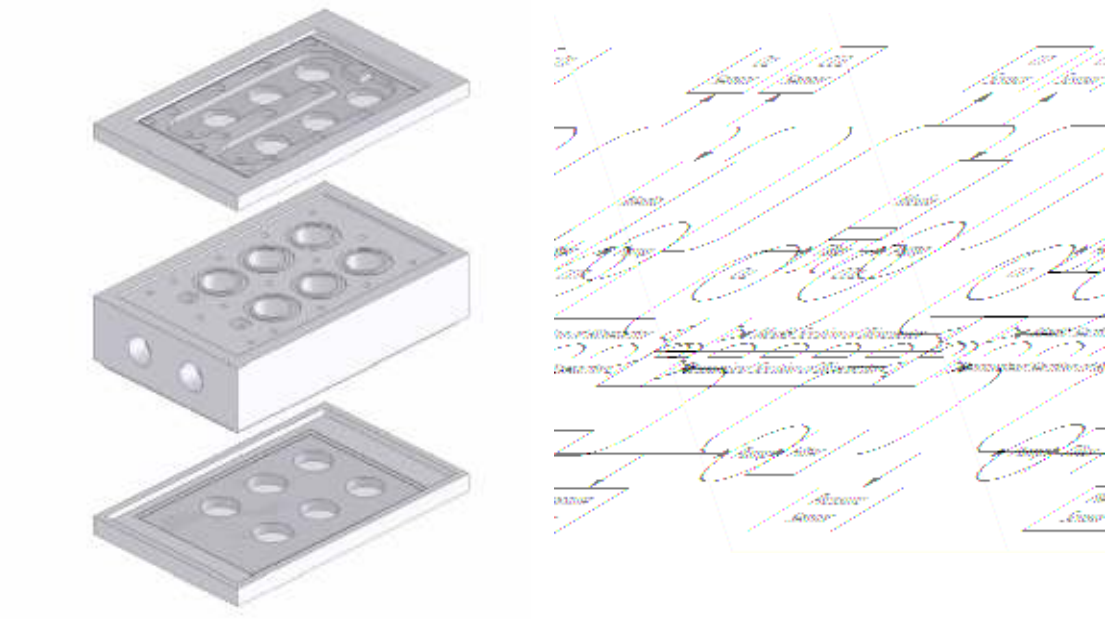

Figure I1.
Exploded view of suggested bioreactor design (left) and ideal closed loop structure for bioreactor system

1.4 Materials Biocompatibility Study

The bioreactor is a complex system involving fluid flow, culture media and control sensing. As described above, its operation is dictated by a number of criteria and a number of variables must be considered in its design.
An appropriate solution must factor the material properties of its components into the design of a suitable bioreactor. The main criteria for suitable materials are that they be biocompatible, sterilizable and easily machinable [7].

A number of materials were tested in the survey study performed by Shah and Voorhees [7]. These materials were chosen on the basis of their behavior in biocompatibility studies and implant applications in a variety of other settings. The materials studied were polyetheretherketone (PEEK), polyoxymethylene homopolymer (POM-h), polytetrafluoroethylene (PTFE), ultra high molecular weight polyethylene (UHMWPE),

titanium and stainless steel. These materials have been successfully employed in the past as implant materials [9] [10] [11] [12] [13]. To determine the cytocompatibility of the materials in the study, Shah and Voorhees used two cell culture techniques –a *cytotoxicity configuration* test and a *growth inhibition* test. The former consists of a standard method of measuring the cytotoxicity of materials in direct contact with cells in monoloayer, where the cells are grown and the material is placed on top of the cells. In the second technique, the cells are seeded in the presence of the material from the beginning of the process.

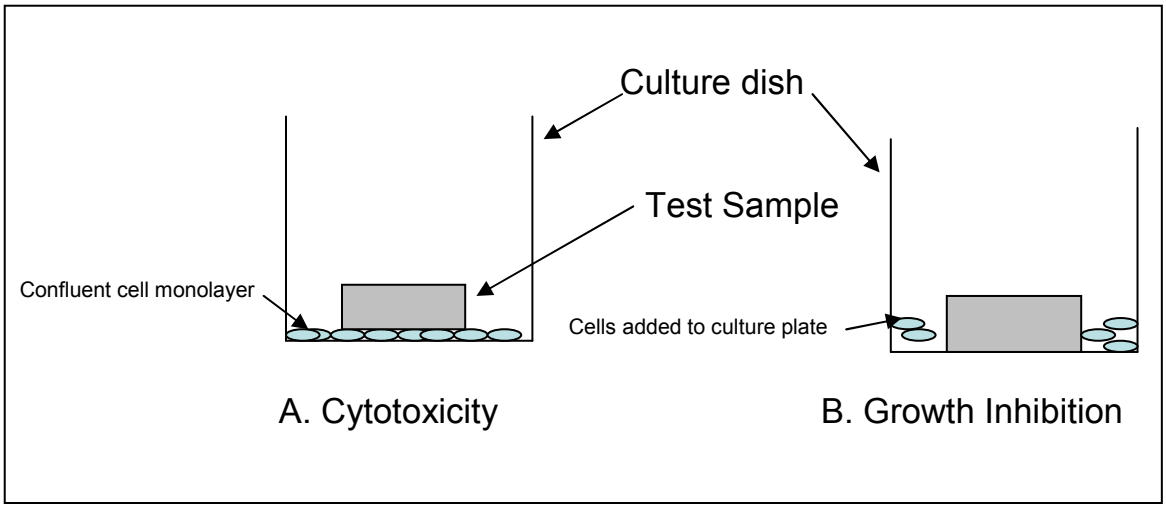

Figure I2. Schematic representation of culture techniques used in Shah, Voorhees study (Diagram borrowed from [7])

They concluded that some of these materials in this list were more suited to this application than others. In particular, they found that they found that several of the component materials caused mechanical trauma to the cell monolayer and severely inhibited the growth of cells. They suggested that the factors that contributed to cell trauma and growth inhibition were the following: the cell culture techniques used, the number of autoclave cycles carried out on the materials, and the materials preparation procedures.

The materials preparation procedures involve the following processes: rinsing with water, grinding, ultrasonic cleaning in ethanol and acetone and autoclaving. Shah and Voorhees observed noticeable differences in the biocompatibility of the samples depending on how much treatment was executed on the material prior to biocompatibility testing. For example, POM-h was observed to have increased cytocompatibility after repeated autoclave cycles, while the cytocompatibility of POM-c actually decreased. The actual physical and chemical effects of the autoclave on the surface of the material is not known, and so it is difficult to predict the reason for this unusual behavior. Possible effects of autoclaving include the release of toxic monomers from the polymeric matrix, as in the case of polyethylene terephthalate (PET) [14], or oxidation as in the case of UHMWPE [15] or a reduction in the biocompatibility of a metal like titanium [16]. However, these are only guesses at best, and a detailed study is clearly in order.

1.5 Goal of thesis

The goal of this thesis project is to develop a sound understanding of the chemical and physical effects of the materials treatment process on the polymers used in the study by Shah and Voorhees. In order to do this, it is essential to track the effects of each stage of preparation on the polymer surface and attempt to relate any changes that occur to the effect on cell confluence and toxicity. The polymers investigated in this study are PEEK, POM-h, POM-c, PTFE and UHMWPE. This study is restricted to polymers over the other substances, e.g. titanium, because growth inhibition and cytotoxicity were observed within the subset of the polymers in the research of Shah and Voorhees.

2. Materials

The materials in this study have all previously been used for a variety of biomedical applications. It is important to begin this study with a quick look at the general properties of these materials, their past performance in the biomedical field and the results of any toxicity studies performed on them, if applicable.

2.1 Polytetrafluoroethylene (PTFE)

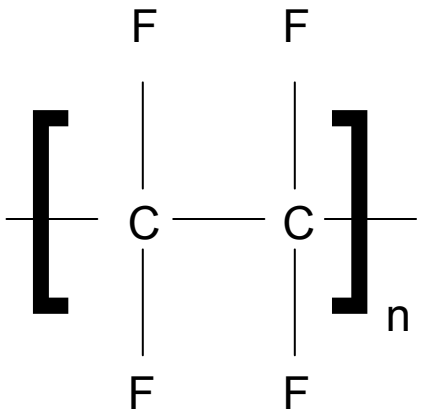

Figure M1. Chemical Structure of PTFE.

Traditionally, polytetrafluoroethylene (PTFE) is made from tetrafluoroehylene via an emulsion polymerization reaction under pressure and in the presence of water and a free radical catalyst. It can also be synthesized via fluorination of polyethylene close to room temperature [17]. This polymer is highly crystalline in nature, and can withstand temperatures upto 330°C [18]. Also known as Teflon®, the material has a high density, can resist extreme heat, cold and UV radiation [19]. It also has extremely low absorption abilities (less than 0.01% of water poured on its surface is absorbed) [19]. PTFE has been used in hip replacements until it was replaced by UHMWPE because of concerns over toxicity and wear [10]. However, PTFE has still appeared consistently in biomedical applications such as arterial grafts, because of its superior performance *in vivo* [2].

Shah and Voorhees found PTFE to have toxic effects on human corneal fibroblasts, irrespective of the treatment carried out on the material, and they suggest that the material's role as a control be discontinued [7]. Similarly, LaIuppa et al discovered that PTFE was toxic to hematopoietic progenitor cells [20]. It appears that PTFE is clearly an unsuitable candidate for this application, although it has qualities that make it desirable for other reasons (i.e. it is able to withstand heat and has a low absorption). PTFE is still used in the current study since this analysis might be useful to recommend it for other applications.

2.2 Ultra High Molecular Weight Polyethylene (UHMWPE)

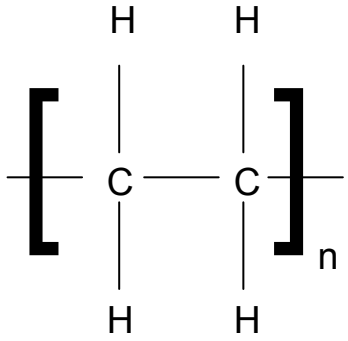

Figure M2. Chemical Structure of UHMWPE.

Ultra high Molecular Weight Polyethylene consists of chains of low density polyethylene bonded together. This low density polyethylene is produced by reacting ethylene gas under pressure in the presence of a peroxide catalyst. The elongated chains of UHMWPE make it less amorphous and more highly crystalline, which reduces its susceptibility to oxidation. UHMWPE is a thermoplastic with a melting temperature of 130°C. It is fairly easy to machine, and is used to make strong fibers called Dyneema and Spectra, which are stronger than steel . UHMWPE is also used extensively for hip and knee joint replacement devices, and is specially strengthened to reduce wear, usually with carbon reinforcements. [21]

UHMWPE has its drawbacks as a biomaterial . If unreinforced, it is susceptible to wear [21]. It breaks down under UV radiation and also has a lower melting temperature than some of the other polymers considered in this study [18]. It cannot be used with the following solvents: benzene, ethylene chloride, methylene chloride, and toluene [19]. Conventional molding processes are not feasible to use in the manipulation of UHMWPE [19]. Furthermore, this material has been found to undergo oxidation during steam sterilization in an investigation by Fuchs et al [15].

In the study that this investigation is based on, UHMWPE was found to cause some mechanical trauma to the cells, but this was thought to be more due to the cell culture configuration than the properties of UHMWPE. There was almost no negative effect on the growth of cells due to the presence of UHMWPE. The slight cytotoxic effect observed after 24 hours of cell culturing was again explained by the culturing technique since the low density of UHMWPE and its placement on the surface of the cell monolayer makes it move around the surface and cause cellular damage. The negative effects of sterilization were not observed by Shah and Voorhees, so it is unclear whether or not this will be a factor in the current study [7].

2.3 Polyoxymethylene (POM-homopolymer and POM-copolymer)

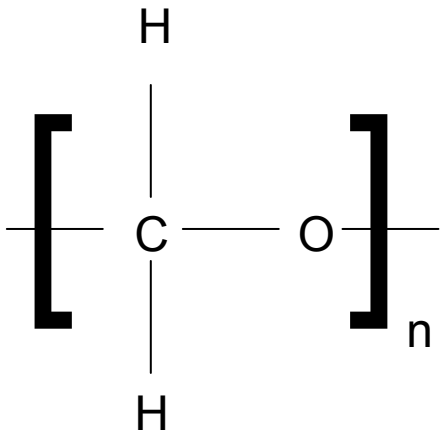

Figure M3. Chemical Structure of POM.

Polyoxymethylene is fabricated from the aldehyde monomer called formaldehyde. There are a number of existing techniques that are use to fabricate this material. For example, gaseous formaldehyde can be condensed onto a cold surface in the presence of metal alkoxides and metal alkyls, Lewis acids and HCl. Then the final product is precipitated out under anionic or cationic conditions in a hydrocarbon solvent. Depending on whether the desired product is the homopolymer or an acetal copolymer, the procedure varies accordingly. [22].

POM-h is commonly referred to as Delrin, whereas the copolymer is called acetal Copolymer. This nomenclature will be used to distinguish the two from here on.

Delrin shares a few common properties with the acetal copolymer. They have similar operating temperatures (between 0 and 85°C) and similar melting points – although acetal copolymer can melt as much as 10-15°C lower than Delrin [18]. This depends on the compounds with which it is reinforced. Acetal copolymer can be reinforced with glass, carbon or PTFE [18]. Both Delrin and the acetal copolymer can be used with relative freedom in solvents that have a pH for between 4 and 9 [19]. They are both relatively susceptible to weather conditions. However, the comopolymer is slightly less absorbing and thus more suited to environments where there is a great deal of moisture. While Delrin is more abrasion resistant, the acetal copolymer is less susceptible to scratching on its surface [19].

Regarding applications, there have been mixed results about the performance of POM, both in its homopolymer and copolymer form. Delrin has been found to perform well in a study by Penick et al that explored its use in a stem cell perfusion bioreactor [9], while LaIuppa et al found that it was toxic to human progenitor cells [20].

In the study done by Shah and Voorhees, the behavior of Delrin was found to be extremely dependent on material preparation, specifically if the material was cleaned with water as opposed to additional cleaning with acetone and ethanol. Delrin cleaned with water had a significantly lowered absorbance measurement in the cytotoxicity test. The copolymer also had a higher growth inhibition and cytotoxicity than all other samples in the investigation. The autoclave cycles had an interesting effect on these samples. Autoclaving was found to improve the compatibility of Delrin that had not be thoroughly cleaned. The copolymer had a decreased cytocompatibility after autoclaving. The authors agree that the behavior of these materials is unpredictable and it is one of the objectives of this study to provide a clearer understanding of the behavior of these POM samples under material handling and autoclaving [7].

2.4 Polyetheretherketone (PEEK)

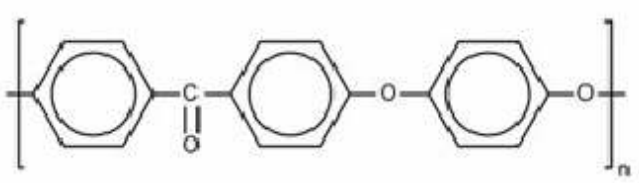

Figure M4. Chemical Structure of PEEK.

(Source for information about PEEK, see [23]).

The features of PEEK as a biomaterial for implants and other medical applications are well documented. The general structure of PEEK is displayed in the above figure. PEEK is a thermoplastic, which means that it can be melted into a liquid if the temperature is high enough and frozen into a glassy state when sufficient cooling is applied. Generically, PEEK is produced by nucleophilic substitution in the reaction of aromatic dihalides and bisphenolate salts. It has a semi crystalline structure, which gives it high resistance to chemical breakdown – it can only be corroded by strongly oxidizing or concentrated anhydrous agents. Mechanically, PEEK performs extremely well – it has a high impact resistance, low wear rate and a low coefficient of friction. It is able to retain these properties over a significant temperature range, from -30°C to 250°C. PEEK can also withstand significant amounts of gamma, X-ray and beta radiation without mechanical breakdown. PEEK has a glass transition temperature of around 143°C.
Due to these properties, PEEK is considered an appropriate candidate for biomedical applications, particularly for prosthetic devices. In particular it has been used in spinal implants.
In previous studies involving sterilization techniques, PEEK has been found to yield satisfactory results. In a study carried out by Godara et al, steam and gamma sterilized PEEK showed only minor changes in its properties and its physical and chemical capabilities remain largely unaffected by the process [24]. In the study by Shah and Voorhees where cells were grown in its presence, PEEK was one of the best performers in that the cell growth was uninhibited. It was also significantly stable under the

autoclave conditions imposed by the experimenters. On the basis of its behavior it was selected for preliminary bioreactor design [7]. Similar results are expected in this investigation.

3. Surface analysis techniques

An examination of the physical and chemical properties of the polymers was made after every step of the preparation procedure to trace the chemical and physical impact of the preparation on the material surface. There are a variety of tools that could potentially fulfill this function, and each of these needs to be considered.

It is important to begin with a consideration of the data that is to be obtained. The data procured at every stage of the materials handling process needs to be of a i)physical and ii) chemical nature, in order to fully describe the state of the sample at that juncture in the process.
The relevant material properties that fall under the physical category are surface roughness, both qualitative and quantitative, and general surface appearance (i.e. how much debris there is on the surface). Chemical examinations are required to gather information on the chemical composition of each polymer, and analyze whether the substance surface changes chemically during its progress through the treatment process.

3.1 Surface roughness, Appearance and Chemical composition

Surface roughness, qualitative surface appearance and chemical composition all have a significant bearing on the biocompatibility of the polymers with the cell growth process. Surface roughness affects cell attachment to the material and the mechanical interaction between the cell monolayer and the material. While cell attachment is not really an important consideration for the fabrication of this bioreactor, it might offer some insights for the group in case a different model for the cell growth procedure is required at some stage. Surface roughness is an important feature to consider in biomedical applications in general since a rougher surface implies that a greater surface area is exposed to the cells or tissues [2]. This can be significant if absorption of culture medium onto the material or cell attachment to the surface is a key part of the process. As mentioned before, this is not necessarily relevant to the particular application being dealt with currently, but these considerations might be relevant at other points in the process.

Surface appearance is important because the presence of debris might cause mechanical trauma to the cells in the monolayer [7] [9] [20] . The chemical makeup of the materials and whether or not they vary as the materials are treated is important since the chemicals produced by these treatments might cause the materials to become cytotoxic. Although the bulk material may be compatible with the cell growth process, debris picked up along the way, or plasticizers and stabilizers added to strengthen the material [2; pp28] or give it certain capabilities might decompose and be the cause of toxicity. Consistent heating might also cause the polymers to approach their glass transition temperatures, softening temperatures or even their glass transition temperatures [2, pp19]. The approach of these temperature limits could fundamentally alter the structure of the polymer, and might result in unpredictable behavior during the cell growth process.

Having established the nature of the data required and its relevance to the larger situation, it is possible to perform a thorough examination of the different analysis techniques that are available. The following table provides a preview of the techniques to be considered.

Physical analysis technique		**Chemical Analysis technique**	
Technique	**Measurement**	**Technique**	**Measurement**
Atomic Force Microscopy	Quantitative Surface roughness	FT Infra Red Spectroscopy	Chemical composition
Profilometry	Quantitative Surface roughness	Energy Dispersive X-Ray Spectrometry	Concentration and mapping of surface chemical composition
Scanning Electron Microscopy	Surface Appearance		
Optical Microscopy	Surface Appearance		
Contact angle	Quantitative Surface roughness		

Table A.1 Techniques considered for study

The selection of the right combination of tests is a vital part of this study. The measurements of the tests should agree with one another to a certain extent, the test should be feasible given the samples in the study, and the tests should be chosen so that the maximum information can be garnered so that this study can be as conclusive as possible.

3. 2 Atomic Force Microscopy (AFM)

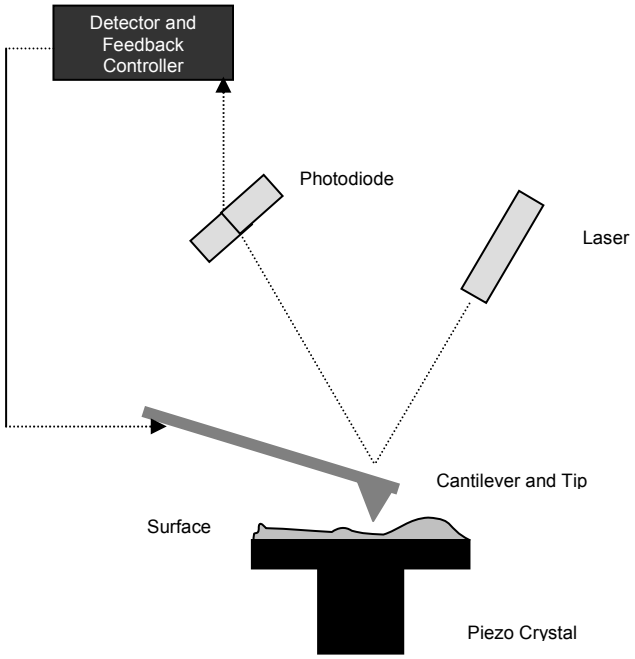

Figure A1. Schematic description of AFM operation.

AFM belongs to the larger subset of scanning probe microscopy. A cantilever with a sharp tip at the end scans over the sample surface. The distance between the tip and the sample is maintained by a feedback loop. The AFM can be operated in several different modes, the most popular being contact mode and tapping mode. For reasons that will become obvious, tapping mode is more appropriate of surface characterization of the polymers in this study. In contact mode, the force between the tip and the surface is kept constant by maintaining a constant deflection as the tip is dragged over the sample. In tapping mode, there is minimal mechanical interaction between the tip and surface. The cantilever to which the tip is attached is oscillated at its resonant frequency using a piezoelectric crystal. Typically, the tip oscillates at a frequency between 50 to 500kHz. Measurements of the changes in oscillation that occur as the tip briefly encounters the sample provide information about the surface. When the tip passes over a bump in the surface, it has less room to oscillate and does so at a lower amplitude, and when it passes over a depression, it vibrates with a greater amplitude since there is more space to do so. These changes are measured as a reduction in the initial set point voltage which controls the oscillation amplitude [25].

Tapping mode would be the more appropriate mode of operation in this case because it minimizes the difficulties that can arise due to tip-sample interaction: friction, electrostatic effects, adhesion between tip and sample that results in sample damage or the creation of topographical artifacts on the sample surface. The physical topography of the sample can be analyzed using this technique. Debris deposited by preparation

processes can be detected using the AFM. A profile of the sample surface can be used to obtain quantitative data on the average surface roughness of the samples.

3.3 Profilometry

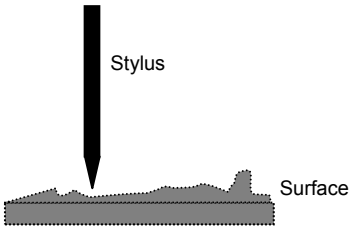

Figure A2. Schematic description of Profilometer operation.

A profilometer measures surface roughness by tracing a profile of the sample surface and transferring the signal to a computer that digitizes the plot for display on a monitor or output to a printer. Profilometers fall into two categories, mechanical and optical. Mechanical profilers raster a stylus (radius 3um) over the sample, and measure average roughness of the sample by averaging over a particular number of points. Mechanical profilometers can operate at a micron resolution. The forces between the stylus and the surface need to be controlled to affect minimum damage to the sample. Typical loading from the stylus can be as low as a milligram and as high as tens of milligrams. The surface must have a limited curvature in order for the profile measurement to be useful.

Optical profilometers use interferometry to measure surface features. Deviations in the fringe pattern produced by reflecting light off the surface are converted to differences in surface height. The advantages of a profiler are the production of a map within seconds and the fact that no sample preparation is necessary. In addition, an optical profiler involves no contact with the sample. The disadvantages of the profilometer measurement are that there are upper limits on the resolution that can be reached. It is difficult to measure samples that have a roughness greater than 1.5um. [26; pp. 699]
A profilometer would be a useful alternative to an AFM measurement, should the sample surfaces prove to be too rough to measure with the AFM probe.

3.4 Scanning Electron Microscopy (SEM)

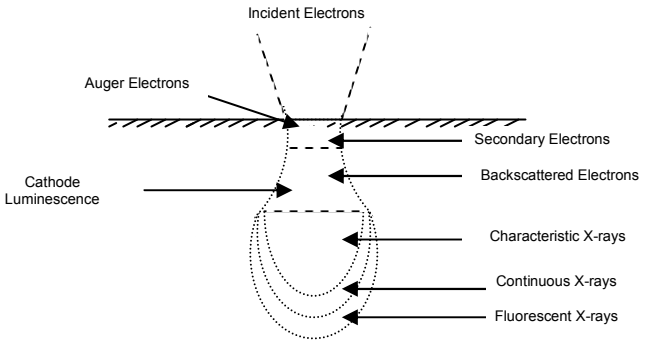

Figure A3. Interaction of SEM incident beam with sample surface.

SEM is useful for producing high resolution images of a sample surface. The SEM is useful to observe physical changes at nanometer resolution that could occur as a result of material handling. An electron beam produced by an electron emitter is directed onto a material surface where it penetrates the sample to a depth that depends on the beam energy. The energetic electrons interact inelastically with electrons from the sample surface. If they impart sufficient energy to the surface electrons so that this energy exceeds the work function of the sample material, the electrons can exit the sample. These electrons are collected at a detector and used to form a picture of the sample [27].
The images produced in the SEM fall into three main categories: secondary electron images, backscattered electron images and X-ray plots that indicate elemental composition. In this section, there is a discussion of the two former modes. The X-ray maps are dealt with in the section on EDS spectroscopy. Secondary electrons and backscattered electrons are produced by highly different mechanisms and are mainly differentiated by their energy. When the energy of the emitted electrons is less than 50eV, they are called secondary. Secondary electrons are emitted mainly from within the first few nm of the surface. When they are produced deeper in the sample, further collisions with other electrons cause them to lose energy and they are unable to escape the sample[27].

Backscattered electrons are higher energy electrons (typically greater than 50eV) that are usually produced deeper within the sample. The energy of backscattered electrons is close to that of the primary electron beam. BSEs are produced more frequently in samples with a high atomic number. Thus samples that are composed of low and high atomic number elements, there is an inherent contrast in the sample image due to BSEs.

The brightness of the image depends on the number of electrons scattered off the sample. Electrons scatter a lot off sharp edges, therefore the image has a 3-D appearance.

The Kirchoff current law holds for the primary electron beam [26, pp. 71]:

$$i_0 = i_{BSE} + i_{SE} + i_{SC}$$

i_0 refers to the primary beam current, i_{SE} refers to the secondary electron current, i_{BSE} refers to the backscattered electron current, i_G refers to the current transmitted through the specimen to ground.
The images formed by these signal complement one another. Amplification of the beam causes each of the above currents to increase. The yield of SE's and BSE's is given by the following relations (obviously compared to the primary beam):

$$\eta = \frac{i_{BSE}}{i_0}$$

$$\delta = \frac{i_{SE}}{i_0}$$

The primary beam energy varies from 0 to 30keV in most commercial electron microscopes. The yield of BSEs, η, increases with atomic number Z, but for a fixed Z, it remains the same for beam energies above 5keV. SE yield δ decreases with increasing beam energy after peaking at a low voltage of around 1keV. The angle of incidence also increases the BSE and SE signal, since more surface interaction can take place. For BSE, this is less prominent since the BSE detector by definition cannot measure forward scattering.

Samples imaged in the SEM are required to be vacuum compatible. Conducting samples are most conducive to SEM techniques, but insulators can be imaged, depending on how insulating they are. Sample charging is a common phenomenon in imaging insulators, and can be reduced by coating the sample with a conducting layer. This is impractical for the purposes of this polymer study because sample coating will alter the surface chemistry and topography, so a solution to this might be to line the polymer surface with copper tape to reduce charging.

3.5 Optical Microscopy

This basic kind of microscopy can be used to observe alterations that may occur on the sample surface on a large scale. These observations will be mainly qualitative, with attempts to note artifacts produced during grinding, or stains that might remain even after the basic clean process.

The microscope available for use in this analyses is one that is typically used in a nanofabrication lab. The microscope is equipped with an incident illuminating unit, i.e. it illuminates the sample from above. The microscope is fitted with a digital camera that contains a 10X objective. In addition, the microscope itself contains a set of 5X, 10X, 20X and 50X objectives. This means that it is possible to get the magnification up to 500X of the sample surface.

The microscope can be operated in one of two modes – bright field or dark field, depending on the nature of the surface being imaged. Usually, bright field microscopy involves a condenser lens situated beneath the stage where the sample is contained. The condenser lens controls the quality of the light delivered to the eye. Light is shone through the condenser, passes through the sample being imaged, is directed through an objective lens and toward the observing eye. The sample absorbs different wavelengths of light depending on its pigmentation and thickness. It is difficult to get a high contrast using bright field microscopy [28].

In the case of epi-illumination (from above the specimen), the objective itself acts as the condenser. A real image of the Condenser Aperture Diaphragm is produced in the plane of the Objective aperture diaphragm, by two additional lenses introduced into the setup for this purpose. This places a virtual diaphragm in that plane. This allows the illuminating cone of light to be matched with the light from the sample point. The luminous field diaphragm is used to dictate the size of the illuminated portion of the sample. The reflector is a semi-transparent glass plate situated below the eye-piece [28].

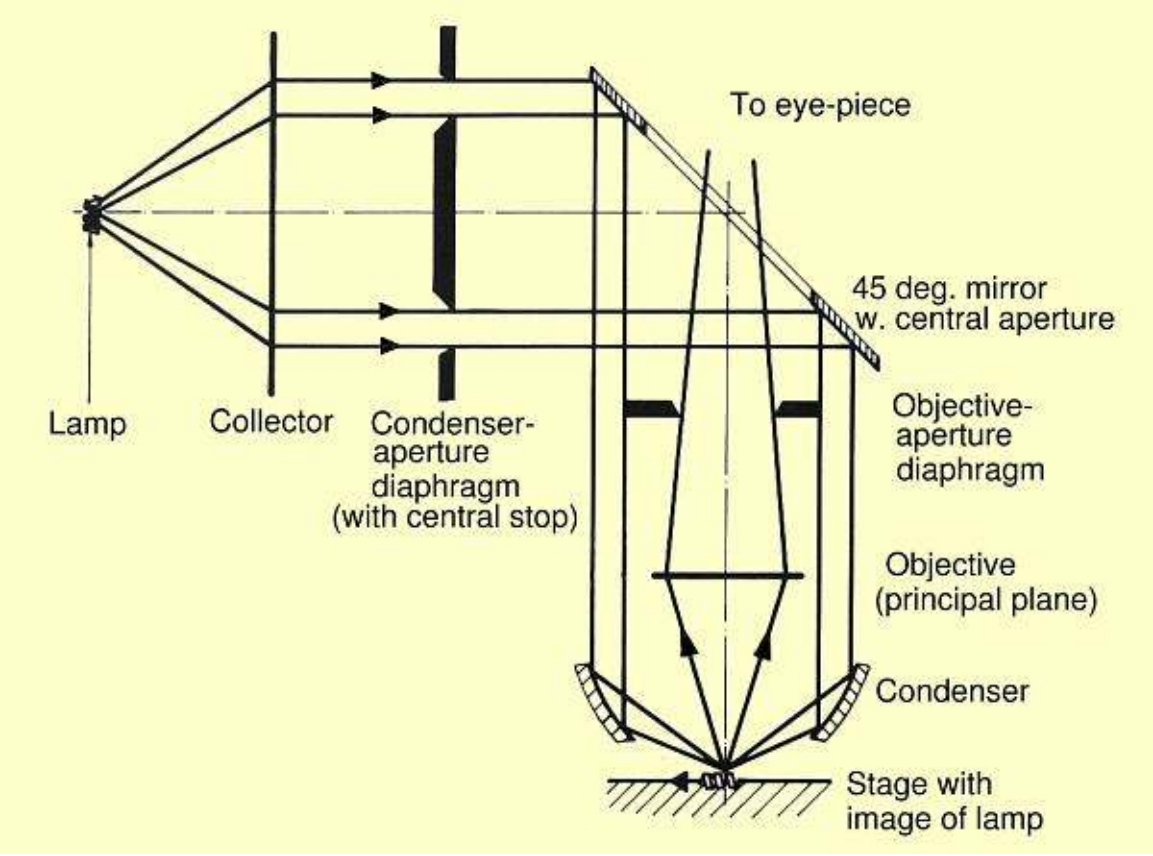

Figure A4. Dark Field Microscopy. (image taken from http://www.nanophys.kth.se/).

Dark field illumination is also possible as a mode for imaging samples. The diagram displays the light path for dark field mode. The collector plate forces the light into a parallel beam. The condenser blocks most of the light, and then most of the light is then reflected by a mirror which allows only a small beam of light through a hole in its center. Another mirror then focuses the light onto the sample. Irregularities on the sample surface deflect the light, and portions of it are directed to the eye of the operator [28].

In this mode, only light that is scattered by the specimen can be observed, making smooth, reflective surfaces appear dark A higher intensity light is required since most of it is scattered. In some cases, the incident volume of light might be sufficient to damage the sample. In this study, dark field microscopy would more appropriate since the samples are relatively rough and opaque in nature.

3.6 Fourier-Transform Infra-Red Spectroscopy (FT-IR)

This kind of spectroscopy is used to identify a compound, or determine the composition of an unknown sample. A beam of infra-red light is directed onto a sample and the quantity of energy absorbed at each wavelength is noted. A fourier transform is used to measure all the wavelengths at once. Then an absorbance spectrum is plottedwith intensity vs wavelength or frequency. This indicates which wavelengths resulted in maximum absorption. Absorption takes place according to the kind of bonds present in the sample. The bonds have very specific wavelengths at which they absorb energy. Comparing the plot with a table of bond wavelengths reveals the exact bonds that inhabit the sample.
In case preparation alters the chemical composition of the sample, by oxidation for example, an IR spectrum will indicate the difference in compounds before and after the preparation.

FT-IR machines are configured with an Attenuated Total Reflection crystal for use with opaque surfaces. This forces the incident beam to be totally internally reflected within the crystal and interact several times with the sample surface, strengthening the signal. This is vital since the samples in this experiment are opaque [26, pp 416].

This technique is advantageous as a nondestructive method of obtaining the chemical composition of the sample [26, pp 417]. In addition, the data is fairly easy to procure, which means a large number of samples can be assayed in a short time. This distinguishes FTIR from other methods of spectroscopy, which are either destructive or complex in terms of data acquisition. The software that accompanies the machine enables the recording of specific peaks in the spectra that allow for easy identification of compounds.

3.7 Energy Dispersive X-Ray Spectrometry (EDS)

Energy Dispersive X-Ray Spectrometry works on the following principle: when an atom is bombarded by high energy radiation, an electron from an inner shell is removed. An electron from a higher energy outer shell drops back into the inner shell in order to transfer the atom back into its original ground state. The potential energy lost by this electron is emitted as an X-ray photon. In atoms with a large number of shells, a cascade of transitions occur because every time an electron drops from a higher energy shell to a lower energy shell, it leaves a hole that can be filled by an electron of ever higher potential energy. Thus from a single primary dose of incident radiation, a number of X-ray emissions can occur, resulting in a spectrum that is unique for every element [26].

In terms of X-ray detection, the EDS system consists of a silicon drift detector that is linked to a field effect transistor (FET) which is in turn connected to an amplifier followed by a multi-channel analyzer. The output of the detector is fed into a CRT display that provides a histogram of the number of photons vs. their energy [29]. A discussion of the roles of each component of the system follows:

- SDD detector: A fully depleted thin semiconductor wafer is used to make the SDD. There is a linear arrangement of anodes at the edge with the cathode positioned at the other edge. The electrons generated by the X-rays are drifted towards the anodes by an electric field. The anodes are linked to the FET.
- FET and Amplifier: The FET is the input of a pre-amplifier. The output from the pre-amplifier is fed into an amplifier which raises the signal to a level that can be processed by the multi-channel analyzer.
- Multi-Channel Analyzer: The MCA contains an A-D converter that accepts the signal from the amplifier. To reduce noise detection, the A-D converter contains a discriminator with a set threshold signal. The accepted signal is used to charge a capacitor which is discharged at constant current. The capacitor is attached to a clock that times the discharge. The time of discharge is proportional to the pulse amplitude, and thus the X-ray energy.

The output produced is a plot of signal intensity vs energy. The location of a peak on the spectrum identifies the characteristic X-ray, and thus the particular element. Certain EDS detectors work best for elements with a Z-value greater than 10 since the low energy X-rays are unable to produce energy that can surpass the threshold of the discriminator.

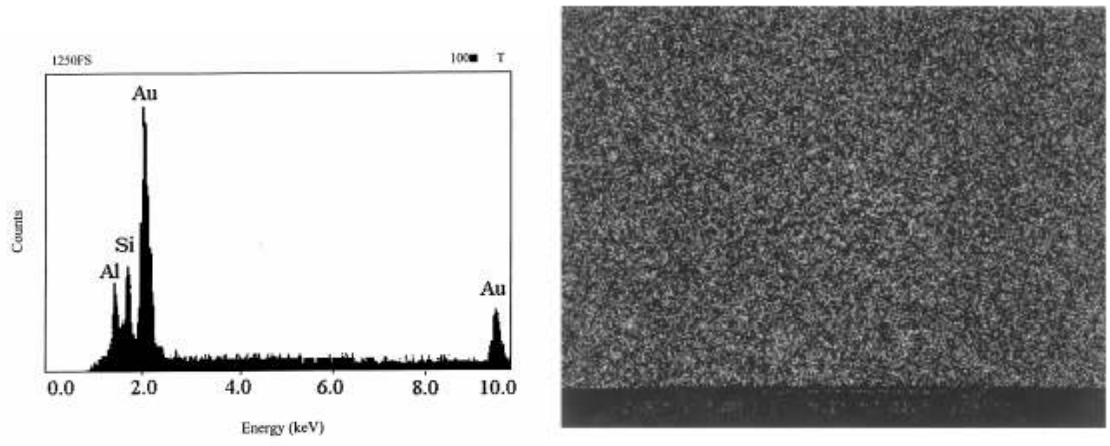

Figure A5. Sample EDS spectrum(left) and elemental mapping of sample surface (right). The sample contains Gold, Silicon and Aluminum.

The EDS system is also capable of producing elemental maps of the sample surface. This displays the location of certain compounds and could be useful for detecting where certain impurities might be concentrated.

The major advantage of an EDS system is that it can be coupled with other detection systems. This is a result of the fact that the EDS system consists of mainly electronic components. The EDS system considered for use in this study is part of an SEM system. A major disadvantage of EDS as a general process is the overlap between peaks that are close. Overlap happens when two peaks of similar amplitude are separated by a distance less than their individual FWHM [26]. This can significantly affect the outcome of an analysis study and means that this technique alone cannot be used in an elemental composition determination of the samples.

Samples to be analyzed by an EDS system can be of any type, as long as they can be pumped down to the vacuum level required by the system. This makes it difficult to image liquids, but this fact is irrelevant to the study at hand. There are problems with excessive charging in non-conducting samples and these might affect the effectiveness of EDS as a technique in this experiment. The roughness of the sample increases absorption of the X-rays, and decreases the accuracy of the spectra plotted. This could also prevent a thorough analysis with EDS.

3.8 Material Wettability

Material wettability is an important concept to observe in this polymer study. Qualitatively, wettability measures the ability of a liquid to bind to the surface of the sample surface under examination. This is important because it provides a means of measuring the amenability of the polymer surface to attachment. Wettability also provides a quantitative measurement of surface roughness.

3.8.1 Contact angle

Wettability is quantitatively summarized by the measure of the contact angle between a liquid droplet and a solid surface. This phenomenon occurs when a liquid drop in contact with a surface does not spread but remains as a drop forming a definite angle of contact at the interface between them [30].

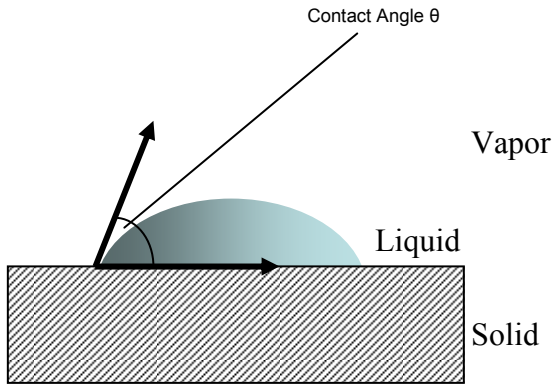

Figure A6. Contact angle representation.

The thermodynamical reasons for this fact are best captured in the following derivation [31]. Consider a drop of liquid on a solid surface. If the area covered by the drop is changed by a small amount ΔA, the Gibbs free energy, ΔG^s, also changes. This change is represented by the relationship:

$$\Delta G^S = \Delta A(\gamma_{SL} - \gamma_{SV}) + \Delta A \gamma_{LV} \cos(\theta - \Delta\theta)$$

where $\Delta\theta$ is the change in the contact angle which goes along with the change in the area, and the other variables represent surface tensions between the solid, liquid and vapor interfaces.

When this system is in equilibrium:

$$\lim_{\Delta A \to 0} \frac{\Delta G^S}{\Delta A} = 0 = \gamma_{SL} - \gamma_{SV} + \gamma_{LV} \cos\theta$$

This is the Young-Dupre equation. Contact angles vary depending on the chemical surface properties of the substance being studied.

3.8.2 Contact angle hysteresis

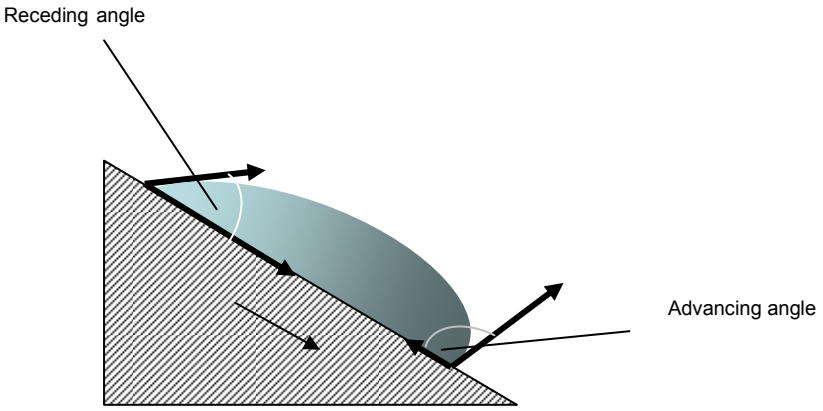

Figure A7. Representation of Contact Angle Hysteresis.

As the liquid advances along a surface, the angle of advance is known to exceed that of the one receding across the surface. Contact angle hysteresis is explained by features of the sample-liquid interaction like surface roughness, surface heterogeneity, solution impurities adsorbance on the sample or changes to the surface caused by the liquid.
Contact angle hysteresis can be explained by the following equation, proposed by Wenzel, which modifies the Young-Dupre equation [32]:

$$r(\gamma_{SV} - \gamma_{SL}) = \gamma_{LV} \cos\theta$$

The coefficient *r* refers to the ratio of the actual surface to the projected geometric surface. Wenzel proposed this relationship based on the fact that a rough surface has a greater area than a smooth one. *r* is a coefficient greater than 1, hence it makes hydrophobic surfaces more hydrophobic and hydrophilic surfaces more hydrophilic.

The measurements of contact angle and hysteresis have a unique theoretical basis and provide relevant information about our sample roughness and material chemistry that can corroborate the results from other techniques. In addition, the experiment is easy to set up from scratch, and requires a fairly simple setup. A groove etched into a metallic plate contains the sample. A drop of water, approximately 3 microliters, is loaded onto the surface and the contact angle noted by video analysis. The plate is then tilted through almost 90 degrees and the point at which the drop starts to move noted. The contact angle hysteresis measurement is made by video analysis of this clip.

3.9 Choice of tests for this study:

Following is a discussion of which tests were used in this study, and the reasons for the selection. A large part of the selection process was dictated by the accessibility of equipment and the time available to use them. For example, the profilometer was not easily accessible, and so could not be employed, although it would have provided useful data.
Also, in the course of the study it was realized that some of the techniques were not appropriate for the selection of materials in this study and so the types of testing had to be reassessed in order to gain the most useful information. This was true in the case of the AFM, which has a range of 6μm for the sample features that it can measure. The artifacts on the samples in the study were too large and fell outside of that range.

Since the samples were autoclaved with steam, it meant that they were in an environment containing a significant amount of water. This meant that they were difficult to pump down in vacuum, which is a prerequisite for imaging with the SEM. This also ruled out the use of the EDS system for this study, since both the EDS and SEM operate on the same machine. Another issue with SEM imaging was that the samples would have to be destroyed. This was a problem because it is desirable to use the same sample to track changes that happen through the process, as opposed to using different samples and analyzing them at various stages. This is an issue because it is difficult to fabricate two samples that are exactly identical. So it would lend much more credibility to the process to use the same sample and avoid destructive tests.

The three forms of analysis that were included in this study were optical microscopy, IR spectroscopy and contact angle measurement.

4. Methods

Following is a description of each part of the materials preparation and analysis procedure

4. 1 Machining

The polymer samples had to be machined from stock rods. The samples were machined to be cylindrical, 0.5 inches in diameter and 0.25 inches in height. The samples were dry-lathed, which means that no oils were added to facilitate the process.

4.2 Grinding

The materials were then ground with silicon carbide sandpaper to ensure a relatively smooth finish on the surface. This was done in stages of 240, 320, 400 and finally 600 grit. The grinding was done by rubbing the surface of the material over the sandpaper with the same smooth motion, to ensure that any grooves created on the material surface were oriented in the same direction. Then the material was rotated 90° and ground over silicon carbide paper of a higher grit in order to smooth out the grooves created by the initial grinding process. In this way, the smoothest possible finish with this technique was obtained.

4.3 Cleaning

a. Rinse with Milli-Q water:

The samples were divided into two groups. The first group of samples was cleaned with a basic procedure of rinsing with milli-Q water three times. Milli-Q water is purified to a high degree by passing it through an ion-exchange unit, which increases its purity by raising its resistance. This is important so that water remaining on the material does not interact electrically with the cells.

b. Sonication with ethanol and acetone

The second group of samples was put through a more thorough cleaning regimen. Samples were rinsed in milli-Q water, then sonicated with acetone for 30 seconds, followed by rinsing for 30 seconds in a bath of ethanol and then rinsed once more in milli-Q water. This was done in order for acetone and ethanol to solvate any oils that remained on the sample surfaces. The sonicating was carried out in the hope that major debris would be shaken off the sample.

4.4 Autoclave:

Both sets of samples were then placed in an autoclave to be sterilized for 30 minutes at 121 C and 30psi. An Eagle Series 3021 autoclave was used. The cycle programmed into the machine allowed the steam to be in the chamber for 30 minutes and then ran a dry cycle for 35 minutes to get rid of most of the residual moisture.

Note: An autoclave works by evacuating a chamber and using high pressure steam to eradicate any bacteria that remains on medical equipment. It is a useful device for sterilization since it operates at a relatively low temperature and kills organisms by denaturing them rather than oxidation. Autoclaving can have detrimental effects on certain hydrolysable materials and polymers. The reaction of the polymers to the autoclave cycle is critical because the materials that form bioreactor components should be able to withstand many autoclave cycles without breaking down chemically or physically. This is important to preserve the longevity of the bioreactor and also ensure that the cell growth is not affected by the bioreactor changes that might occur during the autoclave process. As mentioned in the introduction, previous studies have found that the autoclave process significantly affected the biocompatibility of certain materials.

In this study the materials were autoclaved 1, 5 and 10 times and their chemical and physical attributes compared after these sets of cycles were carried out.

4.5 Analysis

The materials were analyzed with the FT-IR, the Optical Microscope and the contact angle setup at the start and end of each stage of the process. The FT-IR machine used was a Spectrum RX 1 manufactured by PerkinElmer. The spectra measured was averaged over 16 cycles and subtracted from the background.

The optical microscope used consisted of a customized setup built by Prof. Tanenbaum and David Musgraves (Pomona '03). The microscope was set up with a digital Nikon … camera to take pictures of the samples. Sample pictures were taken at 100X and 200X magnification. An image calibration sample with known length of 10 μm was recorded in case measurements of surface features needed to be performed.

The contact angle for the material and the hysteresis effect was also measured using a customized setup. The system was designed in collaboration with David Haley and Glenn Flohr. It consisted of a metallic stage with a machined groove that would hold the sample. A drop of water of 3μl volume was pipetted onto the sample with a micropipette. Then the stage was rotated through 90° and a camera filmed the rotation in order to record the angle at which the hysteresis occurred. There are a number of ways to measure the hysteresis effect (reference). For the purposes of this experiment, the movie made was freeze framed every … of a second and a comparison made between the initial frame, and the frame where the drop first moved.

In order to ensure that the changes on material surfaces were being tracked, it was essential to analyze the effects of treatment on the exact samples. Therefore the same sample of material was taken through the cleaning process, analyzed, autoclaved and then analyzed again after additional autoclave cycles. This eliminated any variability that may have occurred due to differences between material samples, since no two samples are exactly alike in terms of precise surface roughness and debris that might be detected on the sample.

5. Results

5.1 FTIR data

5.1.1 Variation in spectra for similar samples

FTIR data were obtained for three different sets of 10 samples each, at each stage of the materials treatment process. Thus there were at least two spectra representing each particular sample at any given stage of the process. For initial stages, three spectra were recorded, but for the more advanced stages, such as for data after 5 and 10 autoclave cycles, FT-IR analysis was only carried out on two sets of samples. This was mainly due to the time constraints on the project. Having more than one sample is important in order to account for anomalous behavior that might be displayed. Approximately 60 spectral samples were considered for analysis, but only the most significant are actually included in this paper.

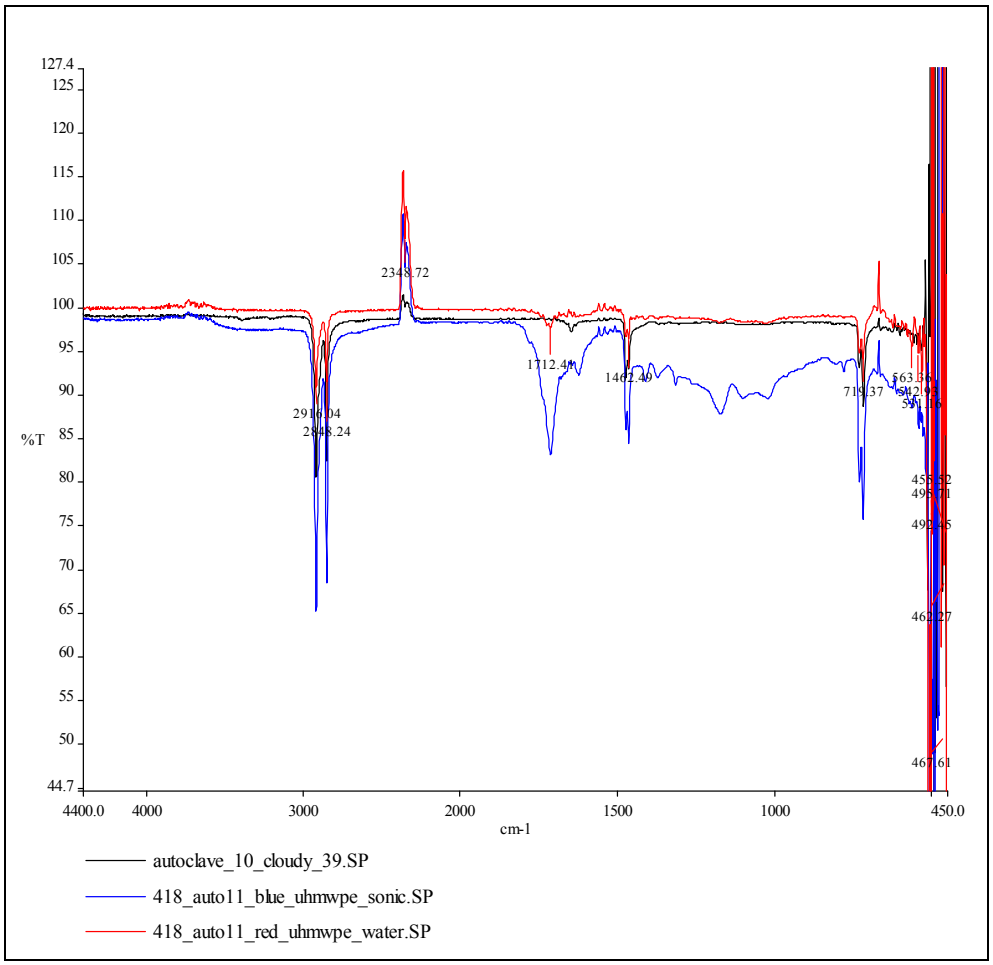

Figure R1. UHMWPE spectra for samples that have undergone 10 autoclave cycles

In the comparison of IR spectra for samples that had undergone exactly the same treatments, the variation in the spectra was negligible, except for the case of UHMWPE that had been autoclaved 10 times (see Figure R1). One of the samples of UHMWPE was severely affected by this autoclaving process and yielded a set of spectra that was significantly different than another sample that had undergone the same treatments. This result will be discussed fully in the next section. For other samples, there was little or no variation in the spectra.

5. 1.2 Functional Groups Detected

Based on the structure of the compounds in the study, the following functional groups were appropriate to search for in the spectra: C-C, C-H, C-O, C=O, C-F, CO_2, H_2O. and the phenyl ring in PEEK. The absorption regions of these bonds are summarized in table R1. This table was used to interpret the peaks in the FTIR spectra. As a starting point, it was important that these bonds were distinguishable in the spectral data, which they subsequently were. This is evident from figure R2.

Bonds present	Absorption region (cm^{-1})
C-C	800-1300 (stretching)
C-H	2800-3000 (stretching) 1300-1500 (scissoring and bending)
C-F	1100-1200
C=O	1680-1800 (stretch)
C-O	1000-1300 (stretch)
Phenyl ring	3000-3100 (stretch) 650-900 (bend) 1600-2000 (fingerprint)
CO_2	2400
	3700-3800
H_2O	1800, 3800

Table R1. Sample spectra for PEEK illustrating functional groups detected
Source: Spectrometric Identification of Organic Compounds, Wiley and Sons, Inc

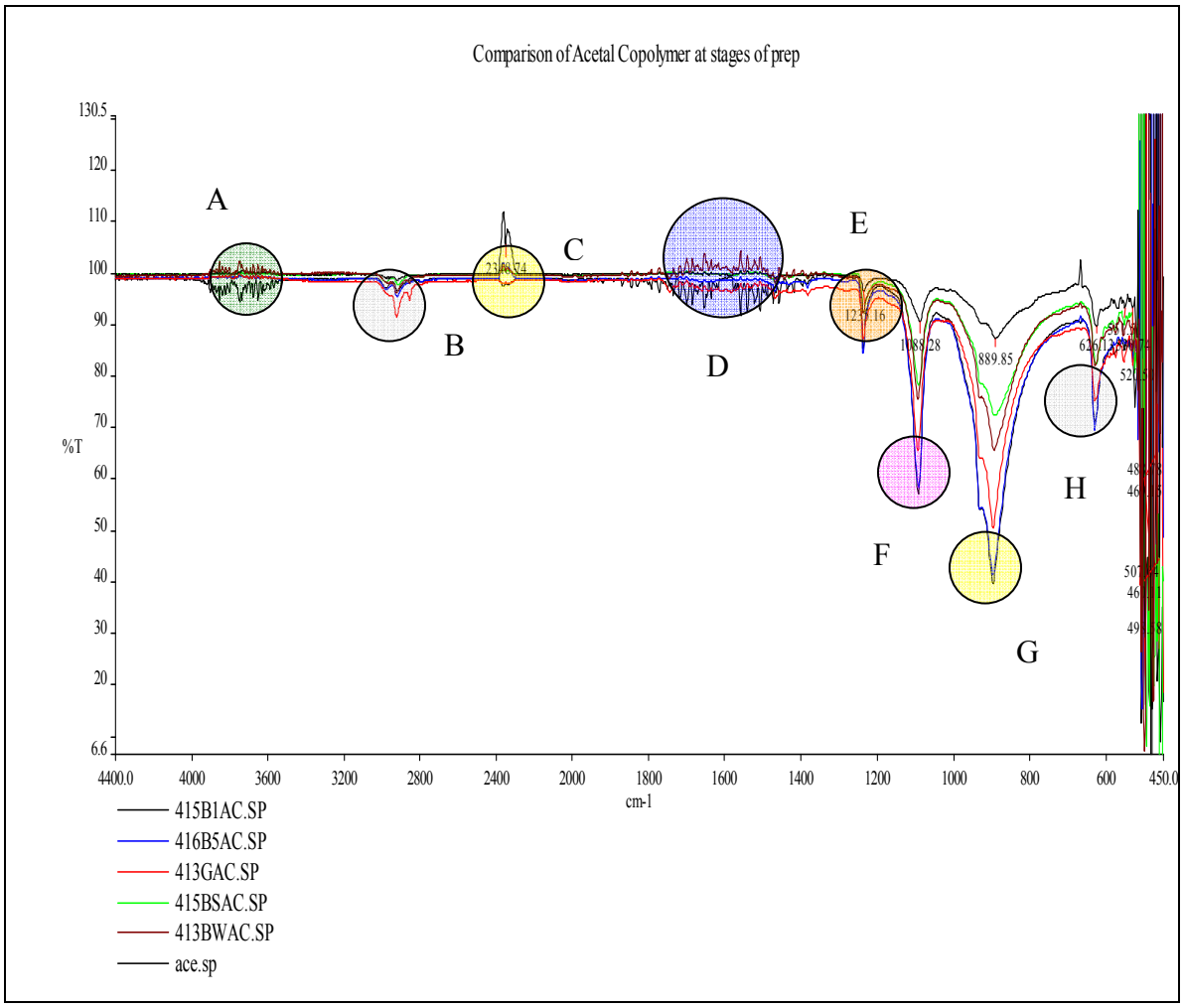

Figure R2. Detection of major functional groups present in sample of Acetal copolymer.

Region	Absorbance (cm^{-1})	Bonds/Compounds present
A	3800-4000	CO_2, H_2O
B	2900-3000	C-H
C	2400	CO_2
D	1500-1700	H_2O
E	1200-1300	C-O
F	1100	C-O
G	900	C-C
H	600	Alkene monomer?

Table R2. Summary of functional groups present in sample above.

One important find was that there was a lot of background noise due to CO_2 and H_2O. It seems probable that H_2O would be present, particularly in the samples that were analyzed post-autoclave. However, a mechanism for the production of CO_2 must clearly be in motion during the autoclave cycles as well, since it is primarily after the autoclave cycles that strong spectra of CO_2 are detected.

5.1.3 Effects of material handling prior to autoclave

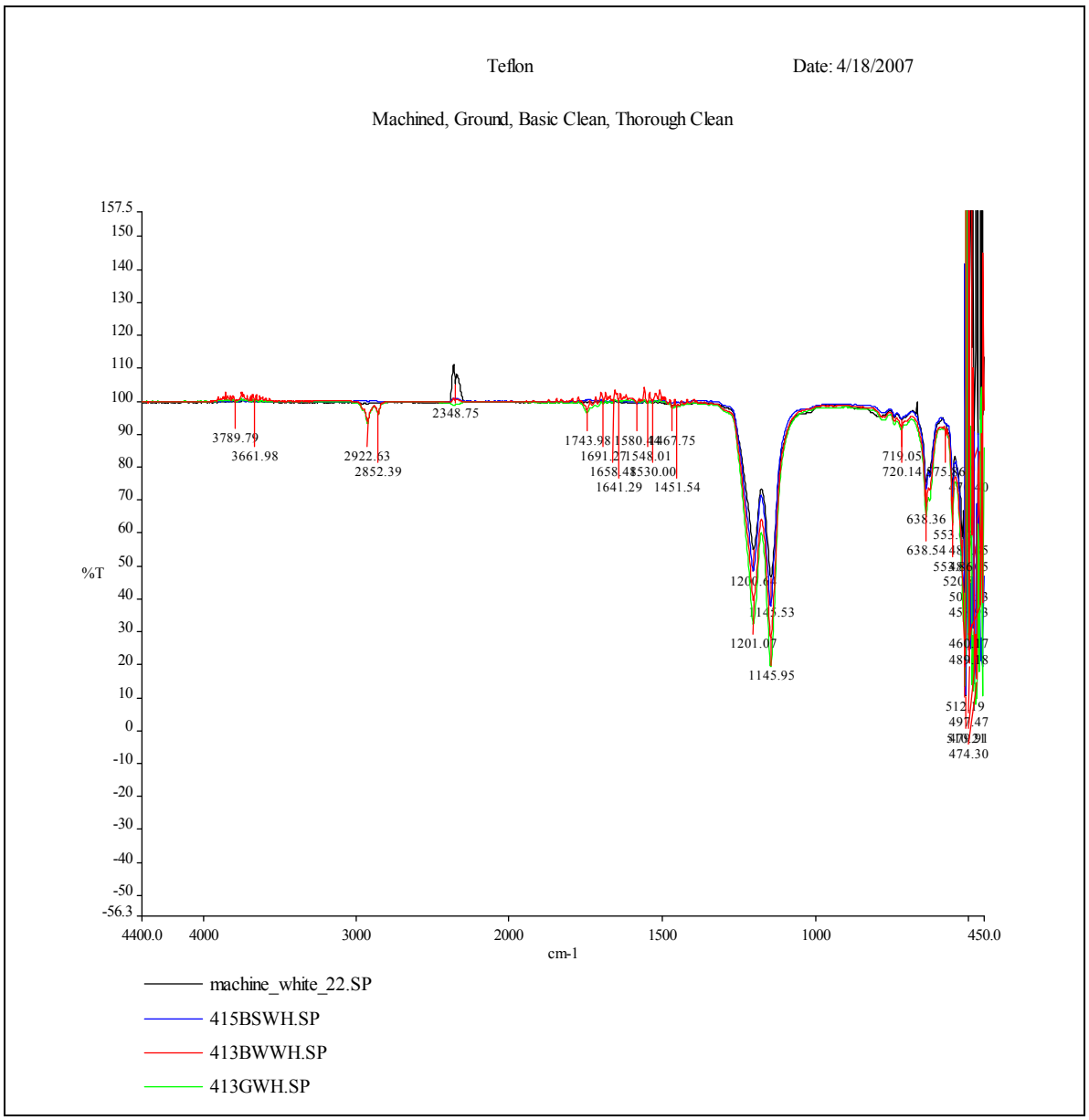

Figure R3. Elimination of CO_2 from FTIR spectra for PTFE

By looking at the data provided by the spectra, it is difficult to conclude the chemical effects of the material handling process, (i.e. grinding, cleaning with water and thorough cleaning) on the samples in the study. Peaks for the major functional groups show up in every spectra and there don't seem to be large scale chemical changes occurring to the polymer. However, for all the polymers there is a great decrease, and in some cases, even an elimination of a peak that occurs at approximately 2400cm^{-1}, in between the machining and the grinding stage. This peak is a standard feature of carbon dioxide spectra, which means that traces of carbon dioxide are being removed in the treatment process before autoclaving.

5.1.4 Comparison of basic clean versus thorough clean

Observations were made on the effects of the basic vs the thorough clean for the autoclave cycles that were carried out. The Acetal Copolymer and Peek showed no differences between the sets of samples for any of the autoclave cycles.

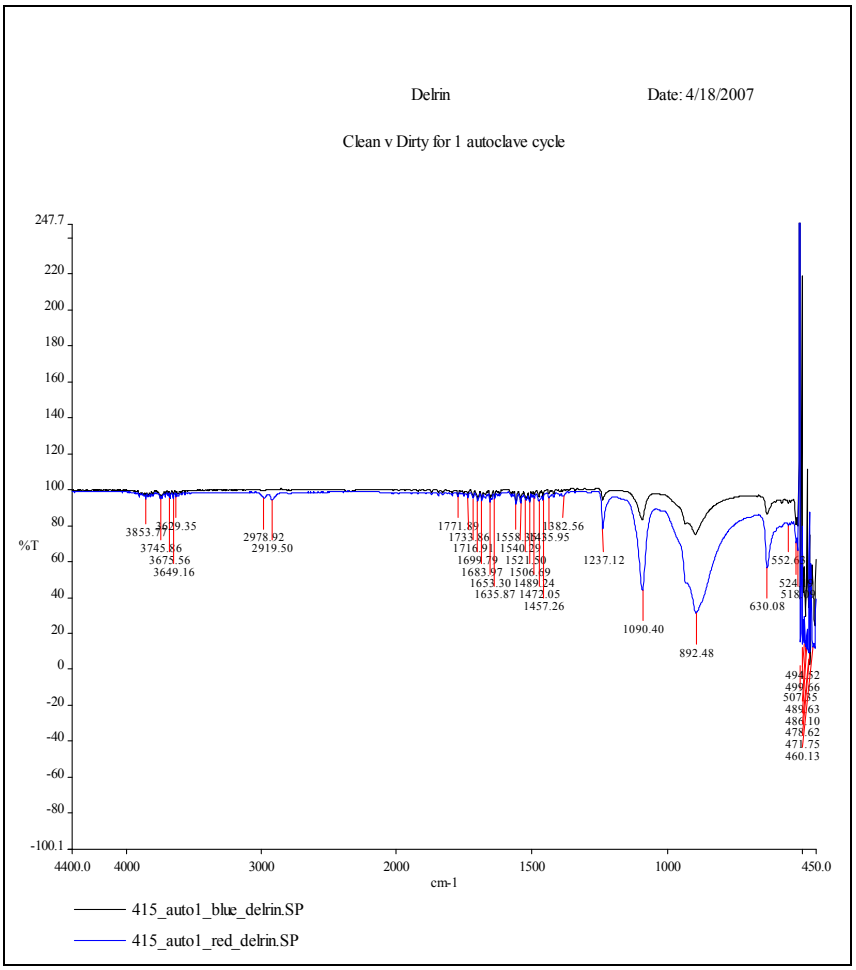

Figure R4. Spectra illustrating unique peak in Delrin sample

For Delrin, there was a pronounced peak at approximately 2900cm^{-1} for the first autoclave cycle with regards to the sample that had been cleaned only with water. The size of this peak wasn't significant enough to be representative of the C-H bond. There was no peak in this case for the sample that had been cleaned. For the samples of Delrin that were analyzed after 5 and 10 cycles, both the clean and 'dirty' samples displayed an absorbance peak at around 2900cm^{-1}. This phenomena will be explored in detail in the following section.

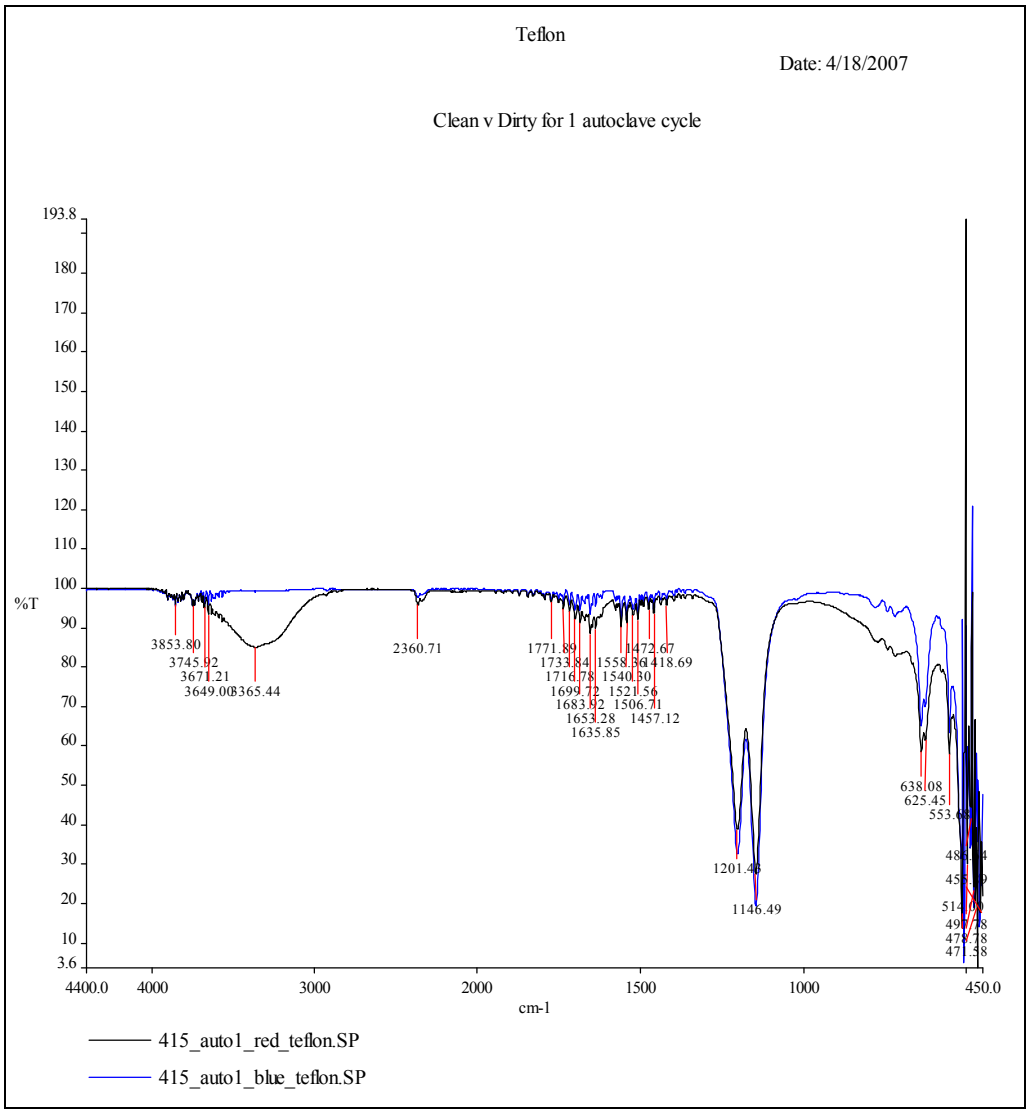

Figure R5. Spectra illustrating unique peak in Teflon sample

For Teflon, there was a unique peak at around 3300cm^{-1} for the sample that had undergone only the basic clean. This peak disappeared when the sample was autoclaved 5 and 10 times.

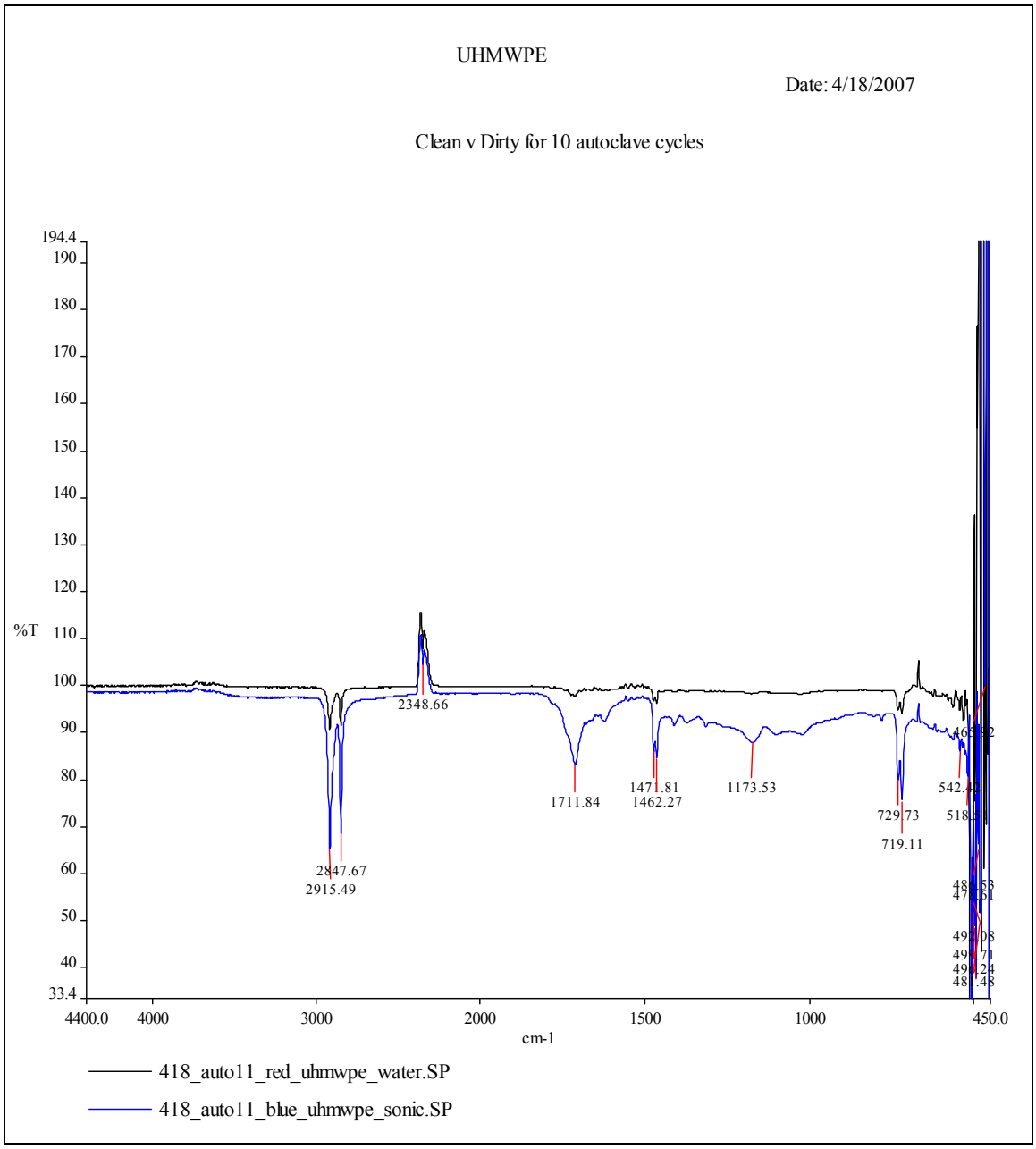

Figure R6. Spectra illustrating peaks in UHMWPE sample

For UHMWPE, there were two distinct peaks that appeared when the dirty sample had been autoclaved 10 times. These distinct peaks were located at 1200cm^{-1} and 1700cm^{-1} approximately.

5.1.5 Dependence on Autoclave Cycle number

Regarding the dependence of the spectra on the number of autoclave cycles, there were no unusual peeks detected for the samples of acetal copolymer and Peek. For the samples of Delrin, as mentioned in the previous section, there were peaks around 2900cm^{-1} that showed up after 5 and 10 autoclave cycles for the sample that had undergone the thorough clean. For Teflon, there was a distinct peak that showed up for one autoclave cycle for the dirty sample – this peak was at 3300cm^{-1} and was not noticed in subsequent analyses. Autoclaving ten times had a clear effect on UHMWPE, which showed a unique peek at 1700cm^{-1} and 1200 cm^{-1}.

In the next section, we will interpret these results and discuss their ramifications in detail.

5.2 Optical Microscopy

There are no particular features that distinguish the materials under the microscope according to their unique chemical composition. The magnification in the image is insufficient to provide any insights into the kind of bonds present or the links between the polymer chains. Hence it is only surface roughness and particular physical artifacts that are detectable via this method.

More than 200 pictures were evaluated in this study, but only the most important have been included in this paper. Qualitatively, the data obtained is what would be expected from such an analysis and is summarized under the following comparisons.

5.2.1 Machining vs Grinding

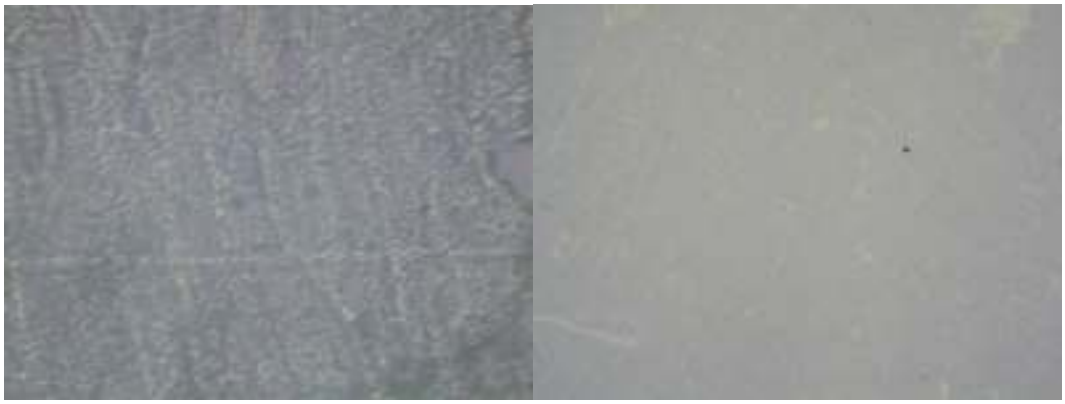

Before Grinding **After Grinding**

Figure R7. Photos illustrating smoothening effect of grinding on sample surface of Delrin

The material surfaces look visibly smoother after the grinding stage in comparison to their appearance after the machining stage. This is true for all the materials in the study. Slight scratches and grooves remain on the surfaces, but a significant portion of the irregularities and indentations seem to be removed by the grinding process.

5.2.2 Grinding vs Basic Clean

Before Basic Clean **After Basic Clean**

Figure R8. Photos illustrating effect of basic clean on sample surface of PTFE

The effect that the basic clean with milli-Q water had was positive for the polymers in the study. However, the amount of debris remaining on the surface for UHMWPE and Acetal Copolymer was only marginally less after this clean, whereas it was more significantly reduced for the other three polymers.

5.2.3 Basic Clean vs Thorough Clean

Basic Clean **Thorough Clean**

Figure R9. Photos illustrating effect of thorough clean on sample surface of PTFE

The response of the materials to the basic clean and the thorough clean was different. For Acetal Copolymer and UHMWPE, the differences observed between the basic clean and the thorough clean were marginal, with only a few extra pieces of debris being removed by the thorough cleaning regimen. For the PEEK there appeared to be qualitatively no difference between the appearance of the surface after the two procedures. However, there was a significant amount of extra debris removed by the thorough cleaning process for Delrin and Teflon.

5.2.4 Effect of Autoclave Cycles

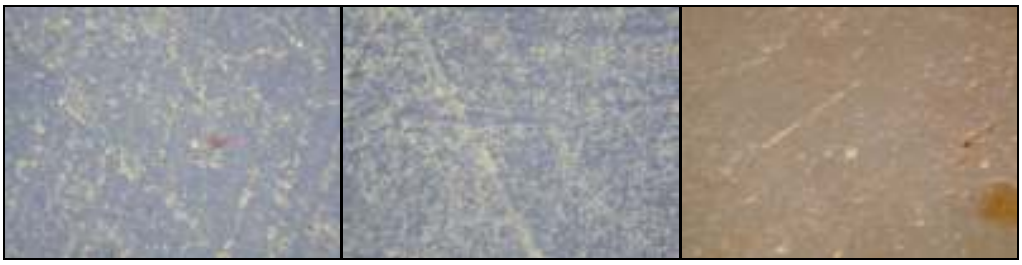

After 1 autoclave cycle **After 5 cycles** **After 10 Cycles**

Figure R10. Photos illustrating effect of autoclave cycles on sample surface of UHMWPE

For all of the polymers except UHMWPE, there are no observable differences in the surface due to the different numbers of autoclave cycles. The surface features look similar and the amount of debris remaining on the surface is comparable irrespective of whether the polymer has been autoclaved 1, 5 or 10 times. For UHMWPE however, there is a marked difference in the appearance of the sample after 10 cycles for both the sample that underwent the basic clean and the thorough clean. This is in comparison to how the material appeared after 5 cycles. Even without the microscope, it is clear that the material surface has been charred and reformed in some way, and it has taken on a brownish tinge from the usual translucent white. Under the microscope, the material appears to have lost some of its pittedness and irregularity and seems somewhat smoother, but with light bumps on the surface.

5.3 Contact angle measurements

Contact angle measurements and contact angle hysteresis data, (i.e. the advancing and receding angles for a sloping surface) were recorded and analyzed for the following cases, based on expected physical changes to the surface.

The general method for calculating the contact angle or the advancing or receding angle were as follows:

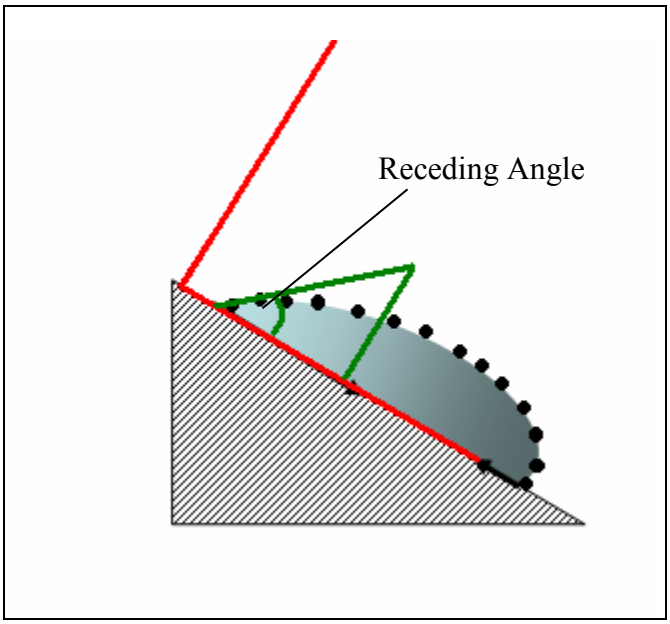

Figure R11. Axes and tangent line superimposed for calculation of receding contact angle.

A photo was taken of the drop on the surface. The photo was imported into Logger Pro software and a set of axes were superimposed onto it. A profile of the curvature of the drop was drawn on the photo. This profile was imported into a graph and the slope of the tangent to the curve was measured. This slope was then evaluated trigonometrically to yield the contact angle for the water on the surface.

This data is summarized below:

Machined Samples

	Acetal Copolymer	Delrin	Teflon	UHMWPE	PEEK
Average	34.10	47.60	74.24	57.74	34.16
Receding angle	19.80	16.71	48.99	32.64	27.94
Advancing angle	30.54	38.68	65.06	43.55	32.23

Ground Samples

	Acetal Copolymer	Delrin	Teflon	UHMWPE	PEEK
Average	5.71	63.93	28.78	5.71	32.99
Receding angle	42.01	26.58	30.13	30.98	26.58
Advancing angle	59.56	59.56	46.96	52.46	58.02

After 1 Autoclave Cycle

	Acetal Copolymer	Delrin	Teflon	UHMWPE	PEEK
Average	64.53	83.64	68.21	48.99	87.94
Receding angle	52.46	35.01	56.34	26.58	42.01
Advancing angle	58.02	47.75	67.41	47.75	68.23

After 10 Autoclave Cycles

	Acetal Copolymer	Delrin	Teflon	UHMWPE	PEEK
Average	63.28	43.21	43.52	28.78	40.02
Receding angle	38.68	42.01	16.71	35.01	30.98
Advancing angle	59.56	79.74	42.01	56.34	50.22

Table R3. Summarized Contact Angle Data

The average angle refers to the average contact angle measured when the stage is horizontal. This angle was measured on two locations on the drop and averaged to yield the final contact angle. Refer to Figure A7 for the details of what the advancing angle and the receding angle are.

5.3.1 Surface Roughness

The results of contact angle measurements are unable to yield significant numerical data regarding surface roughness. This is because the relationship between the true contact angle and surface roughness depends on the interface energy between the solid polymer surface and the liquid used in this technique, i.e. water, by the relationship in Equation :

$$r(\gamma_{SV} - \gamma_{SL}) = \gamma_{LV} \cos\theta$$

Where r refers to the ratio of the actual surface to the geometric surface, the γ terms represent interfacial energies and θ represents the true contact angle, i.e. without any hysteresis involved.

Although the quantities for surface interface energy are not readily available, this measurement was made in the hope that it might yield some useful quantitative data. However, it is evident from looking at the results that no clear conclusions may be drawn from this data since there are a number of variables that need to be accounted for before making any conclusive statements. A fuller explanation will follow in the next section.

5.3.2 Effect of grinding

One would have expected that the contact angle would have decreased after the grinding process since the surface becomes smoother. One would also expect that the material surface chemistry still compensates for some amount of interfacial adhesion, since the surface tension of the water and the bonding in the polymer remains unchanged, even if surface roughness is altered. However, the change in the contact angle for acetal copolymer and for UHMWPE is dramatic. The contact angle actually increases for Delrin and remains almost the same for PEEK. So the response of the materials to grinding with respect to the contact angle is extremely varied.

5.3.3 Effect of autoclaving

Once again, the materials exhibit behavior that doesn't seem to follow a particular trend. Between 1 and 10 autoclave cycles, the contact angle for acetal copolymer stays almost the same, and decreases significantly for all the other polymers in the study. The hysteresis effect too, shows very little semblance of a trend. These are unusual results and imply that the method must be re-evaluated.

6. Discussion

6.1 Behavior of specific Materials

6.1.1 PEEK and Acetal Copolymer (POM-c)

According to the results from this particular study, acetal copolymer and PEEK show no detrimental changes due to autoclaving or materials handling. This agrees somewhat with the results of the study by Shah and Voorhees, in that they too found PEEK to be stable.[7] In their study, acetal copolymer was found to display greater growth inhibition and cytotoxicity after autoclaving, which is not evident from this investigation. One reason for this could be that the autoclave produces a by-product in the copolymer that is activated by the cell culture media. Perhaps this by-product is undetectable by FTIR, which is not an unreasonable idea since the peak could be lost due to overlap with other more prominent peaks in the spectrum. This is a fairly common occurrence when obtaining FTIR data [33].

6.1.2 Delrin (POM-h)

The findings about Delrin could provide some insight into its behavior in the previous study. It is highly possible that the absorbance peak detected at 2900cm^{-1} represents a compound that is responsible for the change in its cytocompatibility as more autoclave cycles are performed on it. This could be the reason that Delrin performed so poorly in the initial studies done in the previous investigation. Further testing needs to be done in order to confirm the nature of the compound that has this particular absorbance peak. The manufacturers state that the operating temperatures for the material are at around 80°C, and since the autoclave is carried out at 40°C higher than that, it could be causing the Delrin to break down and the byproduct to form [19].

6.1.3 PTFE

The behavior of PTFE indicates that a toxic byproduct could be produced when the material is initially autoclaved, but then further autoclaving removes the by product. This explanation is considered in the paper by Shah and Voorhees and would support the fact that a 3300cm^{-1} peak was found after 1 autoclave, but disappeared when further cycles were carried out.

6.1.4 UHMWPE

Finally the behavior of UHMWPE shows that the surface can be chemically and physically affected by the autoclave. This too might be a function of the fact that the operating temperature of the substance is 130°C [19], which is only marginally above the

autoclaving temperature. In fact, it is possible that the melting temperature of the surface is significantly lower than that of the bulk, which would explain the appearance of the UHMWPE after 10 autoclave cycles [surface ref] . It is likely that the substance melted and then reformed. This is part of its properties as a thermoplastic [reference]. It is clear that UHMWPE cannot withstand consistent sterilization with the autoclave.

6. 2 Effects of Material handling and Autoclaving

The positive effects of material handling in the study by Shah and Voorhees could also potentially be explained with evidence from this investigation. The removal of the CO_2 peak from the IR spectra during the process could be the reason why they detected no cycle dependence for the cytotoxicity of their samples – the carbon dioxide was consistently being removed by the thorough cleaning regimen. Also, the thorough clean eliminated some of the material that caused by products to form in the 'dirty' sample of Teflon. Teflon has been found by LaIuppa et al to have toxic effects on hematopoietic progenitor cells. The reason for this, the researchers in that study claim, is leaching of toxins such as plasticizers into the culture media [20]. PTFE is commonly strengthened by filling with other materials such as glass and other resins, so it is possible that one of these fillers is released by the autoclave process [18].

Autoclaving, as predicted, does have some effects on the materials in the study. Repeated autoclave cycles produced an unknown compound in Delrin and partially melted the surface of UHMWPE. The production of this compound in Delrin could be due to the increased temperature over and above its working temperature. In their study, Penick et al suggest that stabilizers and fillers could be the cause of Delrin's cytotoxicity in the study performed by the LaIuppa group [9]. This seems to be another plausible explanation. Penick et al found that Delrin did not have any cytotoxic effects on human mesenchymal cells. They suggest that Delrin's toxicity might be due to cell type sensitivity [9]. However, this explanation is countered by the fact that human corneal cells are extremely robust. Perhaps a chemical study of the cells themselves might provide some insight into this problem.

6.3 Critical Analysis of techniques

6.3.1 FTIR

While FTIR provided the most conclusive information about the samples in comparison to the other tests used in the investigation, there are limitations to this technique. It is possible that spectral peaks from compounds that might be toxic is hidden by noise or overridden by peaks that have a larger amplitude.

Furthermore, it is possible that there exist other mechanisms behind changes to chemical composition of the samples that are not amenable to detection because of the experimental method. For example, in the autoclave, the steam could be reacting with several polymers, but this study has not tracked changes in the autoclave itself. It seems that such an investigation might provide some useful results.

6.3.2 Contact angle measurements

There are many factors that need to be considered when measuring the contact angle of a drop. The size of the drop has significant effects on the measurement of the angle, as presented by Drelich et al. Furthermore, the sample preparation protocol for the contact angle measurement process needs to be well defined. This was not the case with the samples in the study, and thus the measurements were highly erratic. Also, the speed with which the stage is rotated when measuring the hysteresis effect is extremely important since the fluid dynamics are significantly affected (Adamson, 1997). A firm establishment of uniform protocol would have significantly affected the results of this measurement. Ideally, a set of standard contact angle data should also have been procured, but it is evident that the number of factors that contribute to this measurement and the degree to which they affect it is extremely high. The ideal standard would be manufacturer data, but that is not always easily available.

A more accurate method of measuring the contact angle would have been the dynamic Wilhelmy method wherein the sample is immersed in the liquid. The surface tension of the liquid is known and capillary action causes the liquid to rise up on the surface of the solid and keep it vertically afloat [30].

6.3.3 Optical microscopy

The data obtained was satisfactory for the insight it provided and the ease with which it could be procured. It was useful to compare the qualitative appearance of the surface with the data from the contact angle measurements. That provided a good first check on the accuracy of the contact angle measurements. Also, the OM was useful to track the presence of artifacts on the sample surface and whether or not the cleaning procedures were actually making a difference.

7. Conclusions

The following conclusions are derived from this study:

1. PEEK is confirmed as the most suitable polymer in this group for its resistance to chemical and physical attack, and is a good candidate for the bioreactor material. Acetal copolymer also proved to be relatively resistant, however, this fact does not agree with results from the study by Shah and Voorhees.
2. UHMWPE, Delrin and PTFE are all susceptible to physical and chemical changes due to the autoclaving process. The IR spectra for each of them contains absorbance peaks that could represent toxic plasticizers or stabilizers. Further work needs to be done to characterize these peaks and the substances that cause them.
3. This study has confirmed that the materials handling process is an integral part of the study through the effects of the thorough clean over just the basic clean. For Delrin, the thorough cleaning process was found to make a difference when only 1 autoclave cycle was carried out. A peak was detected in the spectra of the sample that had not been thoroughly cleaned. For Teflon, autoclaving produced a peak in the sample that had not been cleaned thoroughly after 1 autoclave as well, but this peak was removed by further autoclaving. For UHMWPE, the difference due to the thorough cleaning regimen was noticeable only after 10 autoclave cycles, when the sample that had not been intensively cleaned was found to be charred.
4. FTIR is a nondestructive and highly informative chemical analysis tool for these polymers, and should be a part of any materials analysis for them.
5. The contact angle measurement technique requires the development of an extensive protocol if the technique is to provide useful quantitative data.

Further suggested work

This study can be taken in a number of different directions, some of which are suggested below.

The contact angle measurement technique can be improved. Either a more sophisticated setup can be developed to incorporate the sessile drop method [30], or a different method for measuring the contact angle can be explored, for example, the Wilhelmy method.

There needs to be an incorporation of other techniques to complement the FTIR and contact angle measurements. A more comprehensive study is in order, particularly involving surface profilometry and EDS data. Mapping the surface of the polymer chemically will provide a lot of useful insight into the changes that occur in the autoclave. Mass spectroscopy could also be used to characterize the polymer before and after treatments, although it is a destructive test. It might be useful to consider studying the effects of autoclave and other treatments on the bulk polymer matrix.

The incorporation of a sensor system into the autoclave would enable monitoring of the chemical state of the polymers as they go through the autoclave process. This might also be a feasible experimental idea to consider.

It would be important to include the cell culture process back into the study. In particular, the culture medium needs to be tested for the leaching of plasticizers or stabilizers from the polymer. This was done in part in the study by LaIuppa et al, where the media was conditioned with the material and effects on the material were noted. In particular an FTIR spectra taken after conditioning the material with the medium would provide useful insight into the chemical interaction between them. Furthermore, the cell culture medium itself could be analyzed under the FTIR or mass spectrometer in order to gauge the chemical makeup of the medium. Understanding this media chemical composition might provide some insights into the interaction between the medium and the polymer.

To summarize: this investigation provided a number of insights into the effects that the materials handling process and the autoclave cycles have on this selection of polymers. However, there is a lot that remains unexplained and more sophisticated and comprehensive study of these phenomena is required in order to fully characterize the effects on the materials in this study.

References

1. Anderson, et al. '*Smart Biomaterials*.' Science, 2004: Vol. 305. no. 5692, pp. 1923 – 1924.
2. Park, et al. Biomaterials, An Introduction, 2nd Edition, 1992 Plenum Press, New York.
3. Tsuruta, Hayashi, et al. Biomedical Applications of Polymeric Materials, 1993 by CRC Press, Inc. pp2.
4. Williams, David. Revisiting the definition of biocompatibility. Medical Device Technology, 2003, vol. 14, issue 8, p 10,
5. Chirila et al. 'Artificial Cornea.' Progress in Poymer Science, Vol 3, Num 3,1998
6. G. Abuksis, S. Orenstein, A. Hershko, R. Michowiz, M. Livne, N. Loia, I. Kremer, C. Winbereger, Cornea recipients: are their opinions and attitudes toward organ donation different from those of the general population?' Transplant. Proc. 36 (2004) 1249.
7. Ajay Shah, Andrew Voorhees, Villapanur Ravi, Elizabeth Orwin, 'Evaluation of Several Materials for Fabrication of a Bioreactor for Corneal Tissue Engineering', Acta Biomaterialia, in press, 2006.
8. Jens Gardner, Philip Amberg, Characterization and Design of Bioreactors for the Growth of Human Corneal Fibroblasts, research report, 2006.
9. Kitsie J. Penick, Luis A. Solchaga, Jim A. Berilla, Jean F. Welter, 'Performance of polyoxymethylene plastic (POM) as a component of a tissue engineering bioreactor', J. Biomed. Mater. Res. A. 75 (2005) 168.
10. F. Escalas, J. Galante, W. Rostoker, 'Biomaterials for total joint replacement', J. Biomed. Mater. Res. 10 (1976) 175.
11. R.R. Richardson, 'Polyamides as biomaterials: preliminary biocompatibility testing', Biomaterials. 14 (1993) 627.
12. S.K. Nelson, J.C. Wataha, P.E. Lockwood, 'Cytotoxicity of dental casting alloys pretreated with biologic solutions', J. Prosthet. Dent. 81 (1999) 715.
13. J.M. Toth, M. Wang, B.T. Estes, J.L. Scifert, H.B. Seim 3rd, A.S. Turner, 'Polyetheretherketone as a biomaterial for spinal applications', Biomaterials. 27 (2006) 324.

14. P.D. Nair, 'Effect of steam sterilization on polyethylene terephthalate',J. Biomater. Appl. 10 (1995) 121.
15. S. Fuchs, S. Linnenbecker, A. Langenbrinck, C. Chylarecki, 'Oxidation of ultra high molecular weight polyethylene as a result of sterilization', Rev. Chir. Orthop. Reparatrice. Appar. Mot. 86 (2000) 15.
16. P.J. Vezeau, G.F. Koorbusch, R.A. Draughn, J.C. Keller, J. Oral. Maxillofac. Surg. 54 (1996) 738.
17. Mike Orthner, Polytetrafluoroethylene/"Teflon" Synthesis, http://www.eng.utah.edu/~nairn/mse/students/MSE3410/Teflon/synthesis.html accessed on April 10 2007.
18. MatWeb Material Property Data, http://www.matweb.com/search/SpecificMaterial.asp?bassnum=O1900 , Accessed on April 20th, 2007.
19. McMaster Catalog, products section, http://www.mcmaster.com/, Accessed on April 20th, 2007.
20. Jennifer A. LaIuppa, Todd A. McAdams, E. Terry Papoutsakis, William M. Miller, "Culture materials affect *ex vivo* expansion of hematopoietic progenitor cells", J. Biomed, Mater. Res. 36 (1997) 347.
21. Kurtz SM, The UHMWPE Handbook, Academic Press, New York, 2004.
22. Machine Design, products section, http://www.machinedesign.com/BDE/materials/bdemat2/bdemat2_3.html, accessed on April 20th, 2007
23. Zeus Inc., technical whitepaper 'Focus on PEEK', 2006.
24. Godara et al., The influence of sterilization processes on the micromechanical properties of carbon-fiber reinforced PEEK composites for bone implant applications, Acta Biomaterialia 3, 2007, 209-230.
25. Prater, C. B. et al. 'Tapping mode Imaging Applications and Technology.' Veeco Instruments, Inc., 2004.
26. Brundle C., Evans Jr. C., Wilson S., 'Encyclopedia of Materials Characterization, Butterworth-Heinemann, 1992.

27. JEOL USA, A Guide to Scanning Microscope Observation, content accessed from http://www.jeol.com/ , on April 20th, 2007.
28. Department of Applied Physics website, 'Section of Nanostructure Physics, http://www.nanophys.kth.se/ , content accessed on April 20th, 2007.
29. Bruker AXS, Working principle – SDD, http://www.bruker-axs.de/ , accessed on April 20th, 2007.
30. Adamson A, Gast A, 'Physical Chemistry of Surfaces, 6th Ed., John Wiley & Sons, Inc., 1997.
31. Jones R, Richards R, 'Polymers at Surfaces and Interfaces, Cambridge University Press, 1999.
32. Wenzel, 'Surface Roughness and Contact Angle, Journal of Physical Chemistry, 1949, accessed via http://pubs.acs.org/cgi-bin/abstract.cgi/jpchax/1949/53/i09/f-pdf/f_j150474a015.pdf?sessid=6006l3, April 20th, 2007.
33. Silverstein R, Bassler C, Spectrometric Identification of Organic Compounds, 2nd Edition, New York, Wiley, 1967.

9. List of figures

9.1 Introduction

9.2 Materials

9.3 Surface Analysis Techniques

9.4 Results

1. UHMWPE spectra for samples that have undergone 10 autoclave cycles
2. Detection of major functional groups present in sample of Acetal copolymer.
3. Elimination of CO_2 from FTIR spectra for PTFE
4. Spectra illustrating unique peak in Delrin sample
5. Spectra illustrating unique peak in Teflon sample
6. Spectra illustrating peaks in UHMWPE sample
7. Photos illustrating smoothening effect of grinding on sample surface of Delrin
8. Photos illustrating effect of basic clean on sample surface of PTFE
9. Photos illustrating effect of thorough clean on sample surface of PTFE
10. Photos illustrating effect of autoclave cycles on sample surface of UHMWPE
11. Axes and tangent line superimposed for calculation of receding contact angle

List of equipment

1. Stock rods of PTFE, UHMWPE, POM-h, POM-c, PEEK, 0.5” in diameter
2. Sheldon M-Series 13” Radius Lathe
3. Silicon Carbide Sandpaper 240, 320, 400, 600 grit.
4. Deionized water
5. Sonicator
6. Ethanol
7. Acetone
8. Perkin Elmer Spectrum RX FTIR Spectrometer
9. Contact angle camera
10. Software
    a. Spectrum for Windows
    b. Imovie for Macintosh
    c. LoggerPro for Macintosh
11. Optical Microscope by Southern Microsystems, with attached Nikon Camera

Acknowledgements

Professors

Dr. David Tanenbaum, Pomona College
My faculty advisor, who has been the mainstay of my education at Pomona and stood by me through it all during my time at Pomona College. I could never repay you for all that you have done for me.

Dr Elizabeth Orwin, Harvey Mudd College
Thank you for taking me into your lab, and working on this project with me, even though you really didn't have to and you had enough students to keep you busy.

Dr. Wayne Steinmetz, Pomona College
Thank you for never turning me away and answering all my many questions.

Dr. Mal Johal, Pomona College
Thank you for your incredible insights about polymers and materials surfaces.

Dr. EJ Crane, Pomona College
Thank you for letting me into the lab after hours, and for lending me your equipment.

Dr. Charles Taylor, Pomona College.
Thank you for always pressing me to be a Chem major, no matter how many times I turned you down.

Dr. Frederick Gray, Pomona College
You've always been an attentive and encouraging presence, ready to drop everything and answer a question or a query. I'm grateful that you came here.

Lab Assistants:

Glenn Flohr, Pomona College
You are the Best. Irreplaceable.

David Haley, Pomona College
You always come through in the clutch. A man for all seasons.

Tom Vasquez, Pomona College
Thank you for letting me use the FTIR, even when I didn't email you in advance.

Elaine Guerra, Harvey Mudd College
Thank you for teaching me how to use the autoclave machine, and for talking to me about your horses.

Students & Friends:

Orwin Lab Group
Thank you for being so welcoming and friendly.

Gordon Whyburn
Thank you for sharing my affinity for all things applied, and for your disdain for people, theoretical physics and astronomy.

Rachel Paterno-Mahler
For being the only girl major in our class, and taking so much stick from all of us. Thank you for your mom, who cooks a delicious meal.

Max 'Carroll' Wainwright
For lending me your theoretical mechanics book during sophomore year, when I couldn't afford to buy my own.

Anand Murugan
For being one of the smartest guys I know. I hope you kick ass in graduate school.

Brett Close
Oh Brett, you old fogey.

Lua Del Campo
You amaze me with your patience. Thank you for taking Systems and Continuum with me.

Erica Nelson
For pulling that crazy all nighter with me on the last day before this was due.

Kevin Kelley
Thank you for teaching me how to read FT-IR spectra.

Vinita Lukose
For allowing me to steal her ID at all hours of the day and night so I could get into the Chemistry building.

Jordan Tong
For being my long suffering roommate and friend.

Chris and Lorraine Harry
For being my surrogate parents in the US. For spending four summers with me.

Praveen Dayananda

For teaching me to love physics my freshman year at Pomona.

Charisse Wu
For teaching me that existence in a superposition of states without collapsing into any one of them can be a beautiful thing. You are the queen of nuance, assumption and critique, and I think you would have made an intelligent scientist.

Nate Calahan
For being as intelligent and loquacious as a friend could wish for.

Avon Fernandes
The only Mangalorean I will ever trust.

Lexie Keller, Maite Rodriguez, David Dilworth, Aaron Boeke
For teaching me that there's more to life than academics.

And last but not least, to my Lord and Savior Jesus Christ, who is able to do more than I could ever hope for, or imagine. Thank you for giving me the opportunity to study Physics and learn about you like I never would have any other way.